The Canadian Mineralogist
Vol. 57, pp. 427-456 (2019)
DOI: 10.3749/canmin.1900003

UNUSUAL MINERAL DIVERSITY IN A HYDROTHERMAL VEIN-TYPE DEPOSIT: THE CLARA MINE, SW GERMANY, AS A TYPE EXAMPLE

GREGOR MARKL[§]

Universität Tübingen, Fachbereich Geowissenschaften, Wilhelmstraße 56, D-72074 Tübingen, Germany

MAXIMILIAN F. KEIM

Technische Universität München, Munich School of Engineering, Lichtenbergstraße 4a, 85748 Garching, Germany

RICHARD BAYERL

Ludwigstrasse 8, 70176 Stuttgart, Germany

ABSTRACT

The Clara baryte-fluorite-(Ag-Cu) mine exploits a polyphase, mainly Jurassic to Cretaceous, hydrothermal unconformity vein-type deposit in the Schwarzwald, SW Germany. It is the type locality for 13 minerals, and more than 400 different mineral species have been described from this occurrence, making it one of the top five localities for mineral diversity on Earth.

The unusual mineral diversity is mainly related to the large number and diversity of secondary, supergene, and low-temperature hydrothermal phases formed from nine different primary ore-gangue associations observed over the last 40 years; these are: chert/quartz-hematite-pyrite-ferberite-scheelite with secondary W-bearing phases; fluorite-arsenide-selenide-uraninite-pyrite with secondary selenides and U-bearing phases (arsenates, oxides, vanadates, sulfates, and others); fluorite-sellaite with secondary Sr- and Mg-bearing phases; baryte-tennantite/tetrahedrite ss-chalcopyrite with secondary Cu arsenates, carbonates, and sulfates; baryte-tennantite/tetrahedrite ss-polybasite/pearceite-chalcopyrite, occasionally accompanied by Ag±Bi±Pb-bearing sulfides with secondary Sb oxides, Cu arsenates, carbonates, and sulfates; baryte-chalcopyrite with secondary Fe- and Cu-phosphates; baryte-pyrite-marcasite-chalcopyrite with secondary Fe- and Cu-sulfates; quartz-galena-gersdorffite-matildite with secondary Pb-, Bi-, Co-, and Ni-bearing phases; and siderite-dolomite-calcite-gypsum/anhydrite-quartz associations.

The first eight associations are of Jurassic to Cretaceous age and are related to at least eight different pulses of hydrothermal fluids (plus the meteoric fluids responsible for supergene oxidation); the last association is of Neogene age. Spatial juxtaposition of the various primary associations produces overlaps of the secondary associations. In addition to natural oxidation processes, two anthropogenic additions led to specific mineral associations: (1) lining of the adit walls with concrete resulted in high-pH assemblages of mainly Ca-rich phases, including arsenates and sulfates; and (2) the addition of hydrofluoric acid to counterbalance the high-pH fluids produced by power plant ashes introduced into the exploited parts of the mine resulted in fluoride assemblages of alkali and alkaline earth metals.

This contribution describes for the first time all types of assemblages and associations observed and physicochemical considerations and models of formation for some of the supergene associations. The meteoric fluids responsible for element mobilization and redistribution, and for the formation of new, secondary phases, interacted with wall rocks prior to and during percolation through the actual hydrothermal associations. Depending on the amount of reaction with ore, gangue, and host rock phases, the chemical composition of the meteoric fluids and its redox potential may vary over short distances. Hence different mineral assemblages and zoned associations record fluid compositional changes, even on the millimeter to centimeter scale. Unusual mineral diversity at the Clara mine therefore develops from a combination of diverse primary hydrothermal mineralization stages, an unusual number of fluid flow events involving compositionally different fluids, and local equilibrium conditions that change within centimeters during supergene processes involving meteoric fluids and anthropogenic additions.

Keywords: Clara mine, fluids, supergene, mineral diversity, hydrothermal, fluid path modelling, weathering, alteration.

[§] *Corresponding author e-mail address*: markl@uni-tuebingen.de

Downloaded from https://pubs.geoscienceworld.org/canmin/article-pdf/57/4/427/4800215/i1499-1276-57-4-427.pdf
by University of Arizona user

Introduction

Today, 5413 different mineral species are known on Earth (IMA list from November 2018), a large part of them being related to supergene oxidation processes of ore deposits. This wealth of supergene mineral diversity reflects subtle changes in the physicochemical conditions of near-surface environments, especially changes in f_{O2}, pH, and metal species activities, which are recorded by varying mineralogical associations in a given deposit or even in a single hand specimen. Hence, these variations in conditions may occur on short time and length scales. The supergene mineral assemblages and associations do not only record these changes, they sometimes (depending on the fluid/rock ratio) also cause or mitigate them (*e.g.*, Ingwersen 1990, Jamieson 2011, Markl *et al.* 2014, Keim & Markl 2015, Keim *et al.* 2016, 2017, 2018a, Reich & Vasconcelos 2015). It is, therefore, of interest to understand in detail why certain supergene mineral assemblages form and what they indicate about the conditions of formation. Furthermore, from a purely curiosity-driven point of view, it is interesting to understand why some (few) localities exhibit an unusually rich mineral diversity, much greater than other similar geological environments. Four famous examples of unusual mineral diversity are the agpaitic magmatic rocks of Lovozero and Khibina, Kola Peninsula, Russia; the Zn-rich metamorphosed skarn deposit of Franklin, New Jersey, USA; the strongly oxidized hydrothermal vein-type deposit of Tsumeb, Namibia; and the multi-stage mineralized hydrothermal Clara vein system in the Schwarzwald, SW Germany. The present contribution will address this last locality.

The Clara mine in SW Germany has been mined discontinuously at least since 1652 and continuously since 1898 (Markl 2015). While baryte was the only important product between 1898 and 1978, fluorite became a second major ore mineral in the 1980s, and since 1997 an ore concentrate of "fahlores" (*i.e.*, tennantite–tetrahedrite solid solutions, which in the following are called "fahlore" for easier reading) and other Cu-Ag sulfides has been produced, from which about 4 t of Ag and about 50 t of Cu are smelted per year (Elsner & Schmitz 2017).

The Clara mine works today at a depth of more than 800 m below surface (corresponding to some tens of meters below sea level) on a gneiss-hosted vein system with three major veins (the baryte vein, in German "Barytgang", the fluorite vein, in German "Fluoritgang", and a quartz-dominated vein running diagonally to the other veins and therefore in German called "Diagonaltrum", Table 1), the first two of which merge at about 850 m below surface. The veins reach the red bed sediments unconformably overlying the gneisses about 50 m below surface, but they fade out in these sediments (Huck 1984, Markl 2015). The veins are up to 10 m wide and produce about 40,000 t of baryte and about 50,000 t of fluorite each year (Elsner & Schmitz 2017). Some primary depth zonation has been described from the baryte vein, where Ag-rich "fahlores" at depths below 450 m below surface are replaced by enargite (Keim *et al.* 2018b) above 450 m below surface. Enargite was first described by Sandberger (1875) and called "clarite", but the Peruvian find and name enargite were given priority. Other primary zonation features are either not present or have not been recognized.

While in the 19th century only a small number of unspectacular baryte and fluorite samples in addition to the above-mentioned "clarite" (= enargite) were collected and transferred to only a handful of mineral collections, miners and mineral collectors started to recognize both the mineral diversity of the supergene phases and the quality of the gangue minerals fluorite (including blue cubes up to 10 cm) and baryte (mainly known as chisel-shaped crystals up to 15 cm) in the 1960s. Since then, tens of thousands of mineral specimens have been collected both underground (by miners) and on the dumps by mineral collectors, rendering the Clara mine one of the best documented mineral localities on Earth. A number of scientists, first and foremost Prof. Kurt Walenta from the University of Stuttgart and Dr. Uwe Kolitsch from the Museum of Natural History in Vienna, have continuously investigated new finds and have described about 460 species from this mine to date (including some minerals from the host rocks, Table ES1[1]), among them 13 type species (labelled with a * in Table ES1). Kolitsch (1997) and Markl (1998) described the possible influence of concrete, which has been used in the mine since about the 1970s, on the formation of specific mineral assemblages, and Pfaff *et al.* (2012) presented a model for the formation of the unusually sellaite-rich parts of the fluorite vein, but apart from these contributions, no attempts have been made so far to describe and explain this unusual mineral diversity in a review-style manner. This is the purpose of the present contribution, which for the first time presents information on characteristic phase assemblages and associations and their setting in the complex vein system (based on many mineral finds of the last 30 years investigated using electron microprobe and XRD), and tries to put these character-

[1] Supplementary Data are available from the Depository of Unpublished data on the MAC website (http://mineralogicalassociation.ca/), document "Clara mine, CM57, 19-00003".

Downloaded from https://pubs.geoscienceworld.org/canmin/article-pdf/57/4/427/4800215/i1499-1276-57-4-427.pdf
by University of Arizona user

istic associations into a spatial, temporal, and thermodynamic context using state-of-the-art geochemical modelling.

Regional Geology

The 50 × 120 km Schwarzwald in SW Germany is a low mountain range consisting of Variscan granites and gneisses which in their eastern parts are overlain by Triassic to Jurassic sediments, mainly Buntsandstein redbeds and Muschelkalk limestones (Geyer & Gwinner 2011). The basement rocks and the Buntsandstein redbed sandstones host more than 1000 hydrothermal veins, mainly composed of baryte, fluorite, and quartz, and containing Pb, Zn, Cu, Ag, Co, Ni, U, Fe, Mn, and Sb ores (Metz *et al*. 1957, Bliedtner & Martin 1986, Steen 2013, Markl 2015, and references therein). About 300 of these veins have been mined over the last 5000 years (Markl 2015). The Clara vein system is one of the largest hydrothermal unconformity-related deposits in the world and it is the last active mine in the Schwarzwald.

Hydrothermal veins in basement rocks and the sedimentary cover in SW Germany formed continuously from about 300 Ma until the present day (Pfaff *et al*. 2009 and references therein, Staude *et al*. 2009, Loges *et al*. 2012a, Walter *et al*. 2016, 2018b). During the last few decades, many different aspects of fluid flow and hydrothermal vein formation have been investigated in the area, including studies on microthermometry (*e.g*., Behr & Gerler 1987, Behr *et al*. 1987, Burisch *et al*. 2016a, Staude *et al*. 2009, 2012a, Fußwinkel *et al*. 2013, Bons *et al*. 2014, Walter *et al*. 2015, 2016, 2017a, b, 2018a), stable and radiogenic isotopes of O, C, H, S, Sr, Pb, Cu, Fe, and Mg (*e.g*., Staude *et al*. 2011, 2012b, Walter *et al*. 2015, 2018a, b and references therein), trace element distribution in "fahlore" and sphalerite (Staude *et al*. 2010, Pfaff *et al*. 2011), paleo-fluid models (Pfaff *et al*. 2010, Staude *et al*. 2011, Fußwinkel *et al*. 2013, Bons *et al*. 2014, Walter *et al*. 2015, 2018a, b), REE-distribution in fluorites (Schwinn & Markl 2005), geochemistry of modern thermal and mineral waters (Stober & Bucher 1999, Loges *et al*. 2012a, Göb *et al*. 2013), leaching experiments on basement and cover rocks (Bucher & Stober 2002, Burisch *et al*. 2016b), modern fluid flow models and hydraulic aquifer properties (Stober & Bucher 2005, Bucher & Stober 2010, Bons *et al*. 2014, Walter *et al*. 2016, 2017a, b, 2018a), and the regional geology (Geyer & Gwinner 2011 and references therein). The recent studies revealed five different mineralization events since the Variscan orogeny, each with distinctive fluid inclusion characteristics. Most of the veins (including the Clara vein) formed due to mixing of hot, basement-derived fluids from depth with shallower, cooler, sediment-derived fluids. The mixed fluids from which the gangue and ore minerals precipitated had a temperature between about 50 and 200 °C. The various observed assemblages, both within a single vein system (like Clara) or in different veins, are related to different sedimentary aquifers taking part in this mixing process, different mixing proportions, and the presence or absence of a reducing agent such as methane or graphite.

Burisch *et al*. (2018) used U-Pb SSI dating of successive hydrothermal carbonates to show that the same vein system can be opened and mineralized several times over millions of years. They also quantified the different consecutive mineral assemblages arising from hydrothermal processes at depth, during erosion, and at near-surface conditions.

This holds especially true for the Clara vein system, where Huck (1984) distinguished five different hydrothermal stages with several substages responsible for the baryte, fluorite-sellaite, and quartz-galena mineralization (Table 2; Fig. 1). The ages of the various mineralization stages have been constrained by sedimentological, Rb-Sr, Sm-Nd, and U-Pb studies (Burisch *et al*. 2018, Huck 1984, Mertz 1987, Walter *et al*. 2018b, Pfaff *et al*. 2009) and it has become obvious that, although most of the mineralization is of Jurassic–Cretaceous age, the structures of the Clara vein system have opened and been mineralized several times from at least the Jurassic (173 ± 2 Ma, Pfaff *et al*. 2009) to the Neogene (mineralizing events at the neighboring Wenzel and Friedrich-Christian mines have been dated at approximately 18.6, 13.7, 8.0, 4.0, and 0.6 Ma, see Walter *et al*. 2018b and Table 2). This information is important to understanding the evolution of the fluid and vein system and the formation of the various primary (hypogene) mineral associations detailed below.

Mineralogy of the Clara Vein System

Primary mineral associations

All mineral phases and assemblages/associations described below and in Table 3, be they primary or secondary, were carefully determined by an appropriate combination of EDX/electron microprobe and μXRD techniques, using either small hand specimens or thin sections. Many hundreds of photographs of the various minerals and their assemblages can be found at mindat.org and in Markl (2015).

Primary mineral associations are those crystallized directly in an open space from hydrothermal fluids at temperatures between 50 and 250 °C (see Walter *et al*. 2016) and which do not replace any older hydrothermal mineralogy. Reactions with host rocks may have occurred during their formation.

Downloaded from https://pubs.geoscienceworld.org/canmin/article-pdf/57/4/427/4800215/i1499-1276-57-4-427.pdf
by University of Arizona user

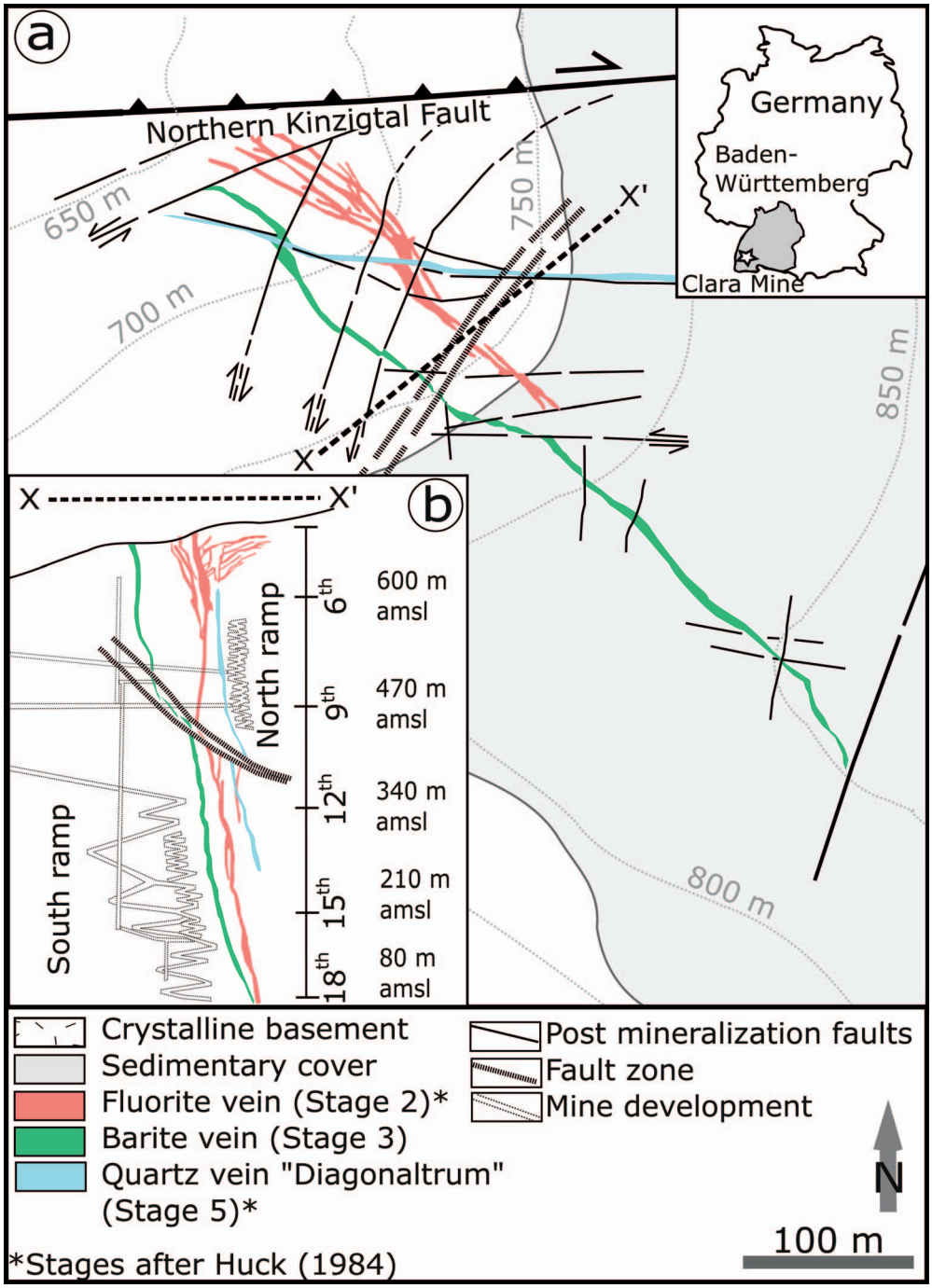

FIG. 1. (a) Geological map of the Clara vein system showing the main hydrothermal stages and major tectonic structures (see text). (b) Cross section of the Clara Mine with the projected mine development. Modified after Huck (1984) and Bucher *et al.* (2009). "m amsl" = meters above median sea level.

Downloaded from https://pubs.geoscienceworld.org/canmin/article-pdf/57/4/427/4800215/i1499-1276-57-4-427.pdf
by University of Arizona user

TABLE 1. GERMAN NAMES USED IN THE TEXT, THEIR ENGLISH TRANSLATION, AND THEIR MEANING

German name	English translation	Explanation
Barytgang	baryte vein	main baryte mineralization in the Clara mine
Diagonaltrum	diagonal vein	important quartz-galena mineralization in a vein diagonal to the baryte and the fluorite vein
Fluoritgang	fluorite vein	main fluorite mineralization in the Clara mine
Scheelitmaterial	scheelite material	scheelite-rich material
Silberspat	silberspar	baryte rich in silver ores
Meißelspat	chiselspar	baryte with a conspicuous shape, like a chisel
Messerspat	knifespar	baryte with a conspicuous shape, like a knife
Honigspat	honeyspar	baryte with a conspicuous colour, like honey
Stinkspat	stinkspar	dark purple fluorite, sometimes "stinks" when crushed
Nordfeld	northern part of the mine	stopes in the northern part of the baryte vein
Südfeld	southern part of the mine	stopes in the southern part of the baryte vein

Based on the papers by Huck (1984), Pfaff *et al*. (2012), Keim *et al*. (2018b), and on our own work, the following distinctive associations can be distinguished, ordered from oldest to youngest (see also Table 2).

(1) Quartz with pyrite, hematite, marcasite, and rare ferberite (stage 1 of Huck 1984).

(2) A fine-grained cherty, reddish quartzite containing minute hematite platelets and roscoelite, ferberite, and scheelite in vugs is veined by quartz-fluorite-baryte assemblages (in German called Scheelitmaterial, *i.e*., scheelite-rich material, not mentioned by Huck 1984).

(3) Fluorite with sellaite, rarely with a "five-element assemblage" of native bismuth, uraninite, nickelskutterudite, rammelsbergite, pyrite, and naumannite (Fluoritgang, Stinkspat, stage 2 of Huck 1984). The sellaite-rich part of this mineralization was investigated in detail by Pfaff *et al*. (2012).

(4) Baryte with botryoidal aggregates of pyrite, marcasite, and chalcopyrite (Barytgang, stage 3 of Huck 1984).

(5a) Dominantly baryte with smaller amounts of quartz, fluorite, and an ore association of Ag-rich "fahlore" (below 450 meters below surface = mbs), enargite (above 450 mbs), and chalcopyrite (stages 3 and 4 of Huck 1984). This is the typical association in the southern part of the baryte vein [Silberspat in German (Table 1), where the ores appear as large masses]. This type of mineralization was investigated in detail by Keim *et al*. (2018b).

(5b) Dominantly baryte with smaller amounts of fluorite, quartz, and chalcopyrite (stages 3 and 4 of Huck 1984). This is the typical association in the northern part of the baryte vein (Nordfeld).

(6) Dominantly quartz with some fluorite and an ore association dominated by Bi-rich galena, chalcopyrite, and some gersdorffite (Diagonaltrum, stage 5 of Huck 1984). This type of mineralization was investigated in detail by Staude *et al*. (2012a).

(7) Various Ca-Mg-Fe carbonates (calcite, siderite, ankerite, dolomite) on quartz-coated host rocks with small amounts of chalcopyrite, sphalerite, and very rare gypsum (present on small fractures cutting all other veins, not mentioned by Huck 1984). This type of mineralization was investigated in detail by Burisch *et al*. (2018).

These eight different types of ore-gangue associations introduced a large variety of elements to the vein system, the most important ones being Ag, Cu, Co, Ni, Fe, Sb, As, Se, U, Bi, Pb, W, V, Cr, S, Mn, Ca, F, Ba, and Mg. This primary inventory was partially modified during various later hydrothermal and supergene events.

Secondary overprint by hydrothermal fluids

Later hydrothermal fluid pulses did not only precipitate new phases in newly opened fractures, they also modified earlier-formed mineralizations. It must be stressed that this is not a supergene or oxidative process, but it is truly hydrothermal and the resulting modified assemblages are still dominated by sulfides and, hence, record reduced redox conditions during their formation. We therefore suggest calling them "secondary hydrothermal assemblages". The most spectacular and variable examples of such secondary hydrothermal assemblages are the Ag- and Bi-bearing sulfosalts resulting from the interaction of later hydrothermal fluids with the primary assemblages P5a and P6 (Table 2).

Downloaded from https://pubs.geoscienceworld.org/canmin/article-pdf/57/4/427/4800215/i1499-1276-57-4-427.pdf
by University of Arizona user

TABLE 2. THE MAIN HYDROTHERMAL GANGUE AND ORE MINERAL ASSOCIATIONS FOUND IN THE CLARA VEIN-TYPE DEPOSIT, WITH AGE CONSTRAINTS (MINERALS IN PARANTHESES IN THE LAST COLUMN ARE THE PHASES USED FOR AGE-DATING)

Main stages according to Huck (1984) and this work	Main ore minerals	Age constraints
P1. Silicification	hematite, pyrite, marcasite	
P2. "Scheelite material"	locally native bismuth, nickelskutterudite, rammelsbergite, uraninite; pyrite, naumannite	173±2 (ferberite)[1]
P3. Fluorite main stage (Fluorite vein in Fig. 1)	pyrite, chalcopyrite, "fahlore", hematite (ferberite)	130±20 (fluorite/baryte)[2]; 143±2 (host rock sericite)[2]
P4. Baryte main stage (Baryte vein in Fig. 1)	pyrite, marcasite, chalcopyrite pyrite, marcasite "fahlore", chalcopyrite chalcopyrite	144±5 (host-rock illite)[2]
P5. Baryte interstage	chalcopyrite, marcasite	
P6. Quartz main stage ("Diagonaltrum" in Fig. 1)	galena, chalcopyrite	
P7. Carbonates	pyrite, chalcopyrite, sphalerite, galena	18.6±0.5,13.7±2.7, 8.0±0.2, 4.0±2, 0.6±0.2 (UbPbSSI on carbonates)[3]

[1] Pfaff *et al.* (2009), [2] Mertz *et al.* (1987), [3] these age data of Walter *et al.* (2018b) are for carbonate assemblages found in the neighboring Wenzel and Friedrich-Christian mines; these carbonate assemblages are texturally and mineralogically identical to those found in the Clara mine.
UPbSSI = U-Pb small scale isochron method.

In the Silberspat (Table 1), primary Ag-bearing "fahlore" reacted with the later fluids and a rich diversity of new sulfosalts formed, the most prominent of which are members of the polybasite–pearceite series which today constitute the most important silver ores. Keim *et al.* (2018b) showed that pyrargyrite-dominated members of the pyrargyrite–proustite series, benjaminite, billingsleyite, acanthite, xanthoconite, pyrostilpnite, stephanite, and freieslebenite belong to this secondary hydrothermal assemblage (Fig. 2). These minerals are interpreted to be secondary hydrothermal (in contrast to supergene in a locally reducing environment), because they are typically interpreted as hydrothermal in many Ag-rich deposits worldwide (*e.g.*, Burisch *et al.* 2019), they typically occur well-crystallized in vugs as crystals and aggregates up to a few millimeters in size, and no oxidized, clearly supergene phase such as arsenates or carbonates accompanies them. Silver-poor "fahlore", arsenopyrite, pyrite, and marcasite are also common members of these secondary hydrothermal associations, and hence a typical (schematical) reaction was probably as follows (see Keim *et al.* 2018b who based their interpretation on extensive textural observations and electron microprobe data):

$$\begin{aligned}&23Cu_7Ag_3(Fe,Zn)(As_1Sb_3)S_{13} + 148Cu^+ \\ &\quad + 43As(OH)_3 + 37Fe^{2+} + 7Zn^{2+} + 184H_2S \\ &\quad + 7.5O_2 \\ &= 30Cu_9Ag_1(Fe,Zn)(As_2Sb_2)S_{13} + 3Ag_{13}Cu_3As_2S_{11} \\ &\quad + 30CuFeS_2 + 9Sb(OH)_3 + 117H_2O + 236H^+\end{aligned}$$

"fahlore" I + fluid phase 1 = "fahlore" II + polybasite–pearceite I + chalcopyrite I + fluid phase 2

Where later Pb-bearing fluids interacted with the Silberspat assemblage (Table 1), galena and Pb-sulfosalts such as jordanite, geocronite, heyrovskyite, diaphorite, and berryite formed. Typically, chalcopyrite, pearceite, and "fahlore" are replaced by late-stage hydrothermal famatinite–luzonite, *e.g.*, by the reaction (Keim *et al.* 2018b)

$$\begin{aligned}&Ag_{16}As_2S_{11} + 6Cu^+ + O_2 + 10H^+ \\ &\quad = 2Cu_3AsS_4 + 16Ag^+ + H_2O + 3H_2S\end{aligned}$$

pearceite + fluid phase 1 = luzonite + fluid phase 2

The Bi- and Ag-bearing galena of primary association 6 reacts with later hydrothermal fluids to form Ag-Bi-Pb-Cu sulfosalts including gustavite, matildite, berryite, pavonite, wittichenite, emplectite, and heyrovsky-

Downloaded from https://pubs.geoscienceworld.org/canmin/article-pdf/57/4/427/4800215/i1499-1276-57-4-427.pdf
by University of Arizona user

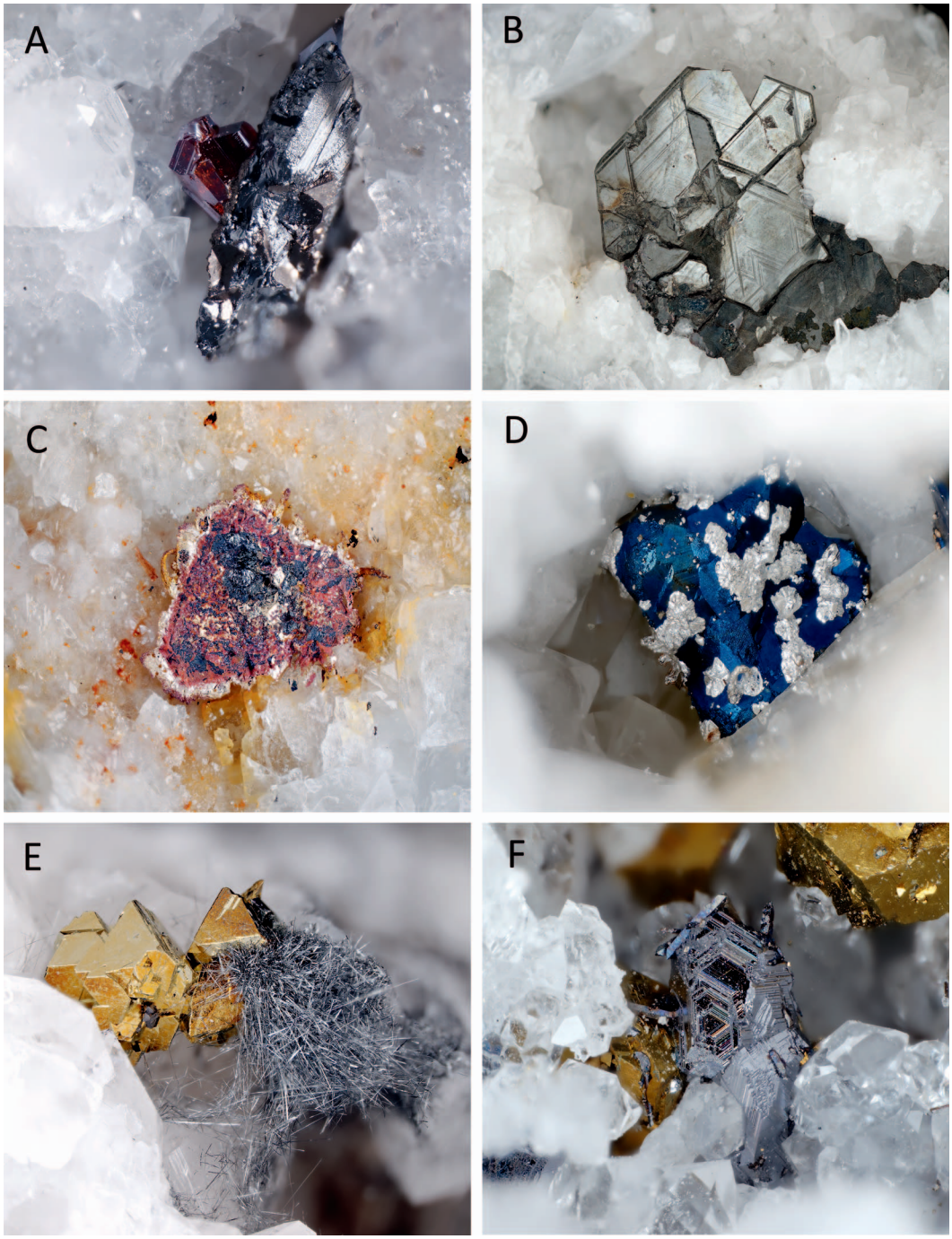

FIG. 2. Secondary silver and bismuth minerals recording modifications of primary hydrothermal mineral assemblages. (a) Pyrostilpnite (red) overgrowing a pearceite crystal. 3 mm. (b) Large pearceite crystal on corroded Ag-bearing "fahlore". 1.5 cm. (c) Native silver, cuprite, and relics of (Ag-poor) "fahlore" recording supergene Ag mobilization. 1 cm. (d) Native silver on "fahlore" crystal covered by blue covellite. 4 mm. (e) Berryite needles on chalcopyrite. 5 mm. (f) Blocky matildite crystals on chalcopyrite. 4 mm.

Downloaded from https://pubs.geoscienceworld.org/canmin/article-pdf/57/4/427/4800215/i1499-1276-57-4-427.pdf
by University of Arizona user

ite. Additionally, cobaltite and stibnite occur in small amounts. Chalcopyrite is a typical member of this association, as is a second generation of (Bi-free) galena. This association closely resembles those described from neighboring mines in Staude *et al.* (2012). The minerals of this assemblage typically form needle-shaped aggregates of millimeter-size which are hard to distinguish from each other. Wittichenite and some matildite occur in blocky crystals, typically in epitactic intergrowth with chalcopyrite or secondary galena (Fig. 2).

Interestingly, the sulfide mineral bismuthinite is not part of this association, but occurs as a later supergene phase together with typical supergene minerals such as cerussite and anglesite. As anglesite was observed in stable coexistence with galena, this may represent a transitional association between reducing and oxidizing conditions.

Secondary overprint by meteoric fluids

Meteoric fluids have entered the Clara vein system upon uplift and erosion more or less continuously since Neogene times (Hautmann & Lippolt 2000). These meteoric fluids were (at their first contact with the vein) both oxidized due to their equilibrium with atmospheric oxygen and undersaturated with respect to all gangue and ore minerals present in the Clara vein. The combination of these conditions led to the dissolution of large parts of the gangue minerals and reprecipitation of at least two generations each of secondary baryte and fluorite with clearly distinctive trace element signatures (Fig. 3; Staude *et al.* 2011, Schwinn & Markl 2005, Loges *et al.* 2012b). While the first (white) generation of hydrothermal baryte (Messerspat, Table 1) contains around 20,000 ppm Sr, the second (yellow) generation of baryte (Honigspat, Table 1) contains around 5000 ppm Sr, and the latest (brown or black, rarely blueish) generation (Meißelspat, Table 1) contains typically around 1000 ppm Sr (Staude *et al.* 2011). Both Honigspat and Meißelspat form crystals up to decimeter size and in the Meißelspat zones these can occur in meter-scale vugs filled with thousands of crystals, commonly of muddy brown or even black color due to small inclusions of clay minerals and/or manganese oxides (Fig. 3). This type of occurrence proves that the third generation of baryte formed at low temperatures in open vugs full of oxidation products or products of erosion and weathering and are, hence, related to the supergene oxidative fluids. The Honigspat may be related to the low-temperature secondary hydrothermal fluids or to early meteoric fluids; this is unclear based on current data.

The other major gangue mineral, fluorite, also shows various generations, the last occurring as typically small, face-rich crystals which have much lower REE contents and strongly negative Ce anomalies in contrast to the primary hydrothermal fluorites (Loges *et al.* 2012b). Their formation is probably related to the supergene oxidative fluids, like the third generation of baryte (Meißelspat, Table 1).

Dissolution or oxidative replacement of hydrothermal sulfides resulted in the formation of supergene oxide, carbonate, arsenate, phosphate, and sulfate minerals containing many different metals, most important of which are Cu, Pb, U, Bi, Sb, Ba, Sr, REE, and Fe. With regard to the eight primary associations from above (Table 2), typical secondary (be they hydrothermal or supergene) associations include (Table 3):

- The Scheelitmaterial (association P2, Tables 1 and 2) gained considerable interest in the 1980s and 1990s due to the occurrence of a rich and rare association of secondary tungstates and vanadium minerals (association SS2). These include cuprotungstite, hydrotungstite, phyllotungstite, hydrokenoelsmoreite, rankachite, and lenoblite (Fig. 4).
- Magnesite and rare celestite in the fluorite-sellaite vein (assemblage P3, Table 2) and unusually diverse supergene uranium phases including torbernite, autunite, nováčekite, uranophane, and many rarities named in Table 3 (association SS3a). Bismuth-bearing phases such as walpurgite, dreyerite, pucherite, schumacherite, or atelestite have also been described from this dark purple Stinkspat (see Table 1 for explanation), but remain rare, similar to Ni-bearing phases like takovite. The occurrence of secondary selenides such as umangite and bohdanowiczite and of native selenium (assemblage SH3) may also be related to this supergene stage; the invariable presence of large quantities of pyrite in the vicinity creates a local reduced environment.
- The massive pyrite-marcasite-chalcopyrite aggregates in some parts of the baryte vein oxidize (both underground and in collections) to a wide variety of Fe- and Cu-sulfates including jarosite, melanterite, chalcanthite, and rarer species such as römerite and rhomboclase (assemblage SS4). These are typically water-soluble. Copper-bearing sulfates such as brochantite, langite, and antlerite (Fig. 4) are locally common; if Cl-bearing fluids are involved, phases such as connellite or lavendulan can form.
- Supergene minerals of association SS5a in the "fahlore"-bearing baryte veins are the ones the Clara mine is most famous for (see Fig. 5). These include colorful Cu minerals such as olivenite, cornwallite, clinoclase, agardite, malachite, and azurite, as well as

Downloaded from https://pubs.geoscienceworld.org/canmin/article-pdf/57/4/427/4800215/i1499-1276-57-4-427.pdf
by University of Arizona user

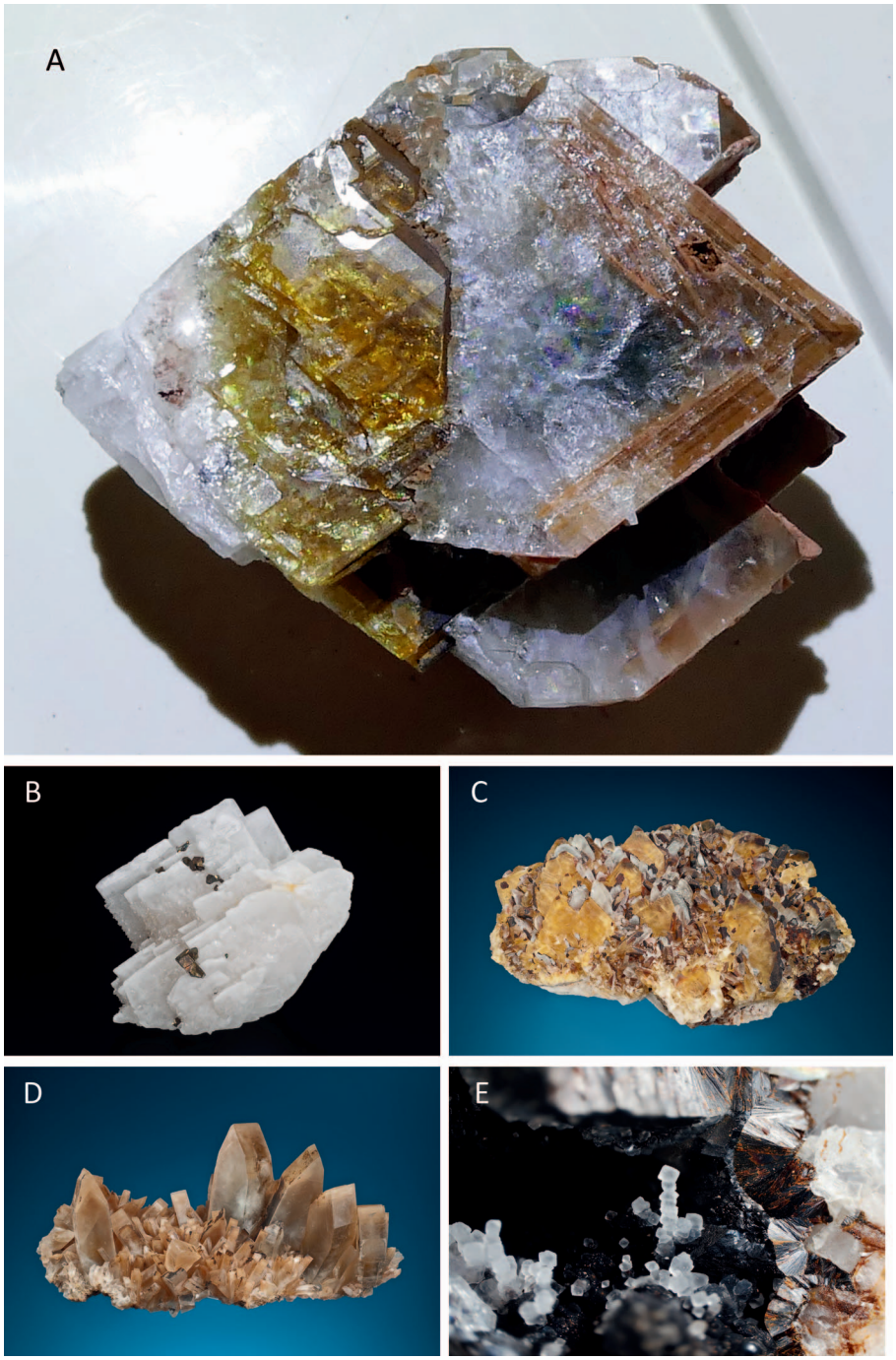

FIG. 3. Gangue minerals as described in the text. (a) Three generations of baryte in one hand specimen: white Messerspat (Table 1), the oldest generation, is overgrown by yellow Honigspat (Table 1) and brown Meißelspat (Table 1). 8 cm. (b) White Messerspat baryte with some chalcopyrite crystals. 7 cm. (c) Yellow Honigspat overgrown by grey Meißelspat. 14 cm. (d) Typical brown Meißelspat in the most common crystal habit. The brown color is caused by minute clay mineral inclusions. 17 cm. (e) Young octahedral fluorite crystals overgrow goethite and, hence, are part of the supergene remobilization of elements. 4 mm.

Downloaded from https://pubs.geoscienceworld.org/canmin/article-pdf/57/4/427/4800215/i1499-1276-57-4-427.pdf
by University of Arizona user

TABLE 3. IMPORTANT SECONDARY MINERAL ASSEMBLAGES OBSERVED IN THE PRESENT STUDY AND DESCRIBED IN THE TEXT

Secondary supergene minerals	Secondary hydrothermal minerals	Primary hydrothermal assemblage
SS2: rankachite, lenoblite, roscoelite, phyllotungstite, hydrokenoelsmoreite, cuprotungstite, bastnäsite, chukhrovite-(Ce), raspite, gasparite-(Ce), anatase, monazite, rutile, brookite	-	**P2:** quartz, ferberite, scheelite, hematite, pyrite
SS3a: magnesite, celestite; locally in 5-element assemblage: takovite, volborthite, annabergite–erythrite, walpurgite, atelestite, dreyerite, schumacherite, clinobisvanite, pucherite, uranophane, torbertnite–zeunerite, autunite, nováčekite, uranotungstite, uranosphaerite, sklodowskite, nollmotzite, ianthinite, schoepite/metaschoepite, francevillite, tyuyamunite, carnotite, rhabdophane-(Ce), wakefieldite-(Ce), torbernite, autunite, nováčekite	**SH3:** native selenium, bohdanowiczite, umangite, guanajuatite	**P3:** fluorite, sellaite, native bismuth, bismuthinite, uraninite, nickelskutterudite, rammelsbergite, pyrite, naumannite, bohdanowiczite, safflorite, emplectite, pavonite, native arsenic
SS3b: zharchikhite, usovite, prosopite, gearksutite	-	**P3:** fluorite
SS4: in mine: langite, posnjakite, brochantite, antlerite, connellite, lavendulan; in collection: römerite, rhomboclase, melanterite, chalcanthite, jarosite,	-	**P4:** baryte, pyrite, marcasite, chalcopyrite
SS5a: native silver, chlorargyrite, bromargyrite, iodargyrite, cervantite, tungstibite, raspite, stolzite, clinoclase, cornwallite, olivenite, scorodite, bariopharmaocisderite, dussertite, crandallite-group minerals (goyazite, gorceixite etc...), conichalcite, chenevixite, arseniosiderite, yukonite, tyrolite, parnauite, posnjakite, langite, devilline; near galena mimetite, bayldonite, mawbyite, duftite, arsenbrackebuschite, "phosphoschultenite", carminite, plumbogummite, cerussite, linarite, tsumcorite, beudantite–segnitite ss, agardite, malachite, azurite, adamite, Cu-rich adamite, tyrolite, brochantite, arsenogorceixite, arsenocrandallite	**SH5a:** native silver, acanthite, freibergite, stromeyerite, mckinstryite, polybasite, pyrargyrite–proustite, pyrostilpnite, matildite, berryite, gustavite, pavonite, wittichenite, emplectite, benjaminite, billingsleyite, galena, famatinite–luzonite, jalpaite, billingsleyite, stibnite	**P5a:** (southern part of the baryte vein): baryte, fluorite, quartz, tennantite–tetrahedrite ss, chalcopyrite, enargite; locally galena, sphalerite, arsenopyrite (the latter locally with gersdorffite and/or cobaltite)
SS5b: goethite, rockbridgeite, dufrénite, kidwellite, cacoxenite, chalkosiderite, beraunite, pseudomalachite, benauite, azurite, malachite, strengite, dufrénite, phosphosiderite, chalcosiderite	-	**P5b:** (northern part of the baryte vein): baryte, fluorite, quartz, siderite, chalcopyrite, arsenopyrite, tennantite–tetrahedrite ss

Downloaded from https://pubs.geoscienceworld.org/cannin/article-pdf/57/4/427/4800215/i1499-1276-57-4-427.pdf
by University of Arizona user

TABLE 3. CONTINUED.

Secondary supergene minerals	Secondary hydrothermal minerals	Primary hydrothermal assemblage
SS5c: native copper, native silver, cuprite, delafossite	-	**P5c:** (baryte vein, unspecified locality): baryte, siderite/ankerite, chalcopyrite
SS5d: claraite, theisite	-	**P5d:** (baryte vein, unspecified locality): baryte, ankerite, chalcopyrite
SS5e: supergene stage 1: cornwallite, olivenite, malachite, azurite; supergene stage 2: ettringite, tenorite, svabite, guérinite, phaunouxite, rauenthalite, calcite, monohydrocalcite	-	**P5e:** (baryte vein, unspecified locality): baryte, chalcopyrite, tennantite–tetrahedrite ss
SS6a: cerussite, anglesite, pyromorphite–mimetite, wulfenite–stolzite, duftite, bayldonite, linarite, caledonite, tsumebite, arsentsumebite, corkite–kintoreite ss, erythrite–annabergite, bismutite, beudantite–segnitite ss, bismuthiite	**SH6:** matildite, gustavite, berryite	**P6:** quartz, baryte, fluorite, Bi-rich galena, chalcopyrite, gersdorffite, tennantite–tetrahedrite ss
SS6b: supergene stage 1: cerussite, anglesite, wulfenite–stolzite, mimetite–pyromorphite, duftite, bayldonite, linarite, caledonite; stage 2: hydrocerussite, leadhillite, susannite, elyite, litharge, massicot, scotlandite	-	**P6:** quartz, baryte, fluorite, Bi-rich galena, chalcopyrite, gersdorffite, tennantite–tetrahedrite ss
-	-	**P7:** calcite, dolomite, ankerite, siderite, gypsum, anhydrite, sphalerite, galena, pyrite, chalcopyrite

Note: The mineral lists of the individual assemblages include only the most important, *i.e.*, selected minerals. ss = solid solution.

Downloaded from https://pubs.geoscienceworld.org/cannin/article-pdf/57/4/427/4800215/i1499-1276-57-4-427.pdf
by University of Arizona user

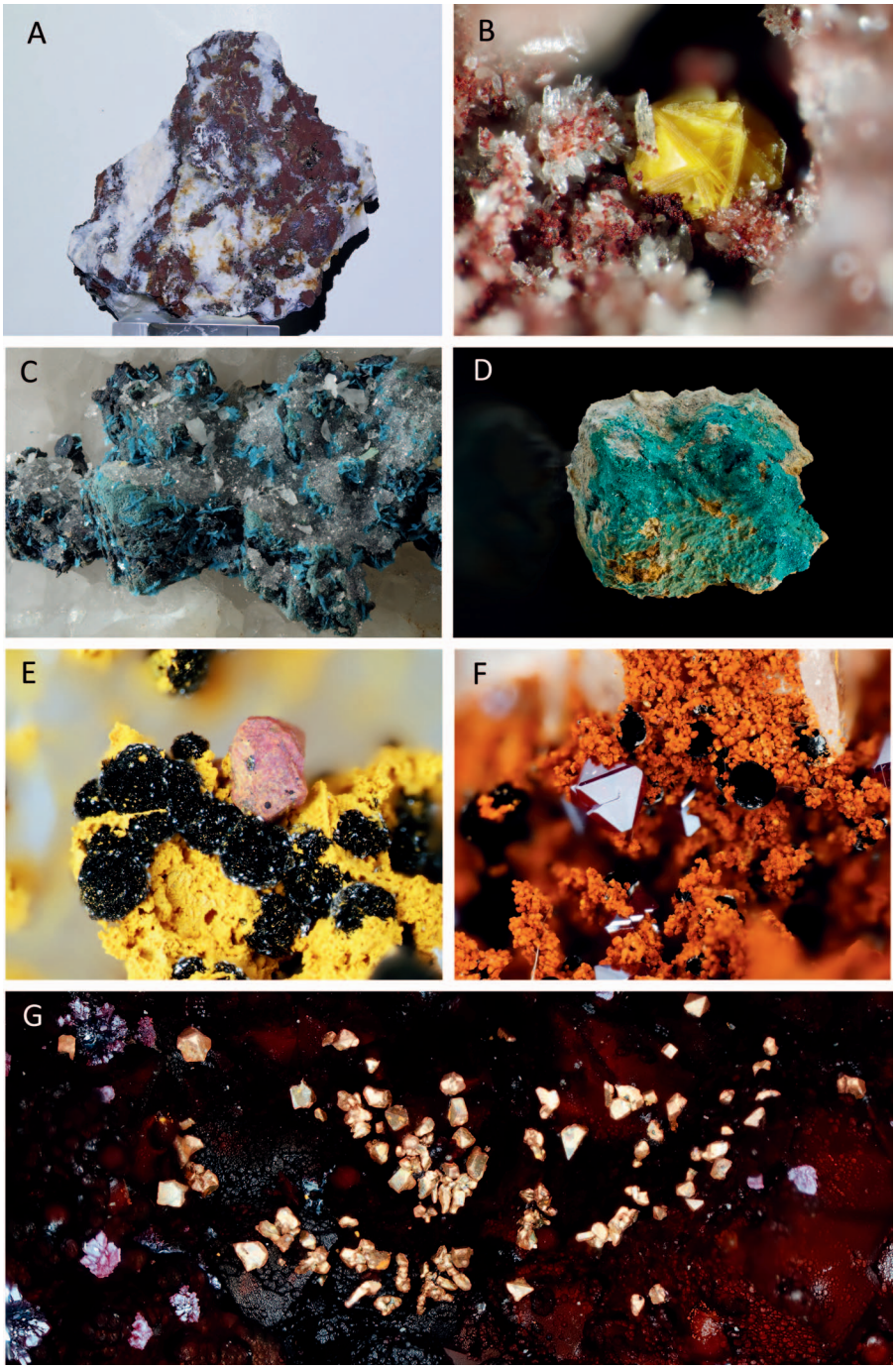

FIG. 4. Various typical mineral assemblages and associations of the Clara deposit as discussed in the text. (a) The Scheelitmaterial is famous among mineral collectors but has never received scientific attention. It consists, as shown, of a reddish drusy chert breccia veined by fluorite, baryte, and quartz. Some of the honey brown material seen is scheelite. 7 cm. (b) Vugs in the reddish chert of the Scheelitmaterial are invariably lined by quartz crystals and contain rare tungsten minerals such as yellow phyllotungstite. 4 mm. (c) Blue posnjakite crystals on "fahlore" crystals. 6 mm. (d) This piece of

Downloaded from https://pubs.geoscienceworld.org/canmin/article-pdf/57/4/427/4800215/i1499-1276-57-4-427.pdf
by University of Arizona user

well-crystallized Fe-bearing arsenates such as scorodite, bariopharmacosiderite, and dussertite (see Table 3). More Zn-dominated assemblages with adamite or Cu-rich adamite were confined to the higher levels, above about 450 mbs. Sulfates or sulfate-arsenates such as langite, brochantite, parnauite, and tyrolite occur only locally, but at all depths. In Ag-rich portions of the vein, native silver and acanthite are typical supergene minerals, sometimes together with chlorargyrite, bromargyrite, and iodargyrite. The oxides tungstibite and cervantite are common secondary phases. Where Pb entered the baryte vein during the secondary hydrothermal overprint, minerals including segnitite, bayldonite, duftite, and carminite appear. The common occurrence of Ba-Sr-Ca-bearing aluminoarsenates of the crandallite group, such as arsenogorceixite or arsenocrandallite, was not reported before the 1980s and it is possible that their formation is related to the anthropogenic effects discussed below.

- "Fahlore"-poor or -free portions of the baryte vein mainly occur in the northern part of the deposit (Nordfeld). Here, decomposition of chalcopyrite led to partly massive aggregates of azurite and malachite with covellite and to the development of an interesting association of Fe and Cu phosphates (association SS5b) which includes rockbridgeite, beraunite, dufrénite, kidwellite, strengite, phosphosiderite, chalcosiderite, and pseudomalachite, as well as rarer Sr phosphates such as benauite (see Table 3). In "fahlore"-free portions of the baryte veins, where siderite or ankerite are present in baryte vugs, two interesting types of assemblages developed upon reaction with Cu-bearing fluids and oxidative destruction of the Fe-bearing carbonate: in the upper levels (above about 400 mbs), native copper-native silver-cuprite-delafossite assemblages formed in the vicinity of goethite pseudomorphs after a former Fe-carbonate mineral (assemblage SS5c; Fig. 4); at one locality in the vein, mined in 1982, an assemblage (SS5d) of claraite, malachite, and theisite formed in the vicinity of partly limonitized ankerite.
- The galena in the Diagonaltrum was altered to produce a wide variety of typical supergene Pb minerals such as cerussite, anglesite, pyromorphite, mimetite, wulfenite, stolzite, caledonite, linarite, bayldonite, duftite, carminite, segnitite, tsumebite, and many more (association 6a; Fig. 5). Malachite and Pb-rich baryte are common phases in these assemblages. This association was enriched with secondary Bi- and Ni-bearing minerals such as bismutite, beyerite, kettnerite, annabergite–erythrite solid solutions, and nickeltsumcorite which resulted from the supergene reactions of gersdorffite and Bi-bearing galena. The secondary hydrothermal phases of assemblage SH6 include Ag-Bi sulfosalts such as matildite and berryite.

Secondary overprint via anthropogenic input

Three types of anthropogenic input have influenced secondary supergene mineral formation in the Clara mine since the 1970s and 1980s. First, the mine walls were systematically stabilized with concrete after about 1970. This introduced Ca-rich material which, upon reaction with mine waters, resulted in the formation of phases like the Ca-sulfate ettringite, which typically occurs with aggregates of tenorite pseudomorphing malachite and with calcite or monohydrocalcite (association SS5e; Fig. 6); young aggregates of Ca arsenates including svabite, phaunouxite, rauenthalite, and guérinite are also most probably related to the interaction of mine waters with concrete, as these phases invariably overgrow earlier supergene phases such as bariopharmacosiderite and scorodite (Fig. 6). Second, in the 1980s the mining company began to fill the empty stopes with ashes from power plants. This material is also highly reactive with mine and meteoric waters, releasing various cations to these waters and increasing the pH significantly. It is, however, not known which elemental concentrations in the analyzed mine waters are due to fluid-ash interaction. This pH increase was in parts so pronounced that—this is the third human interference—hydrofluoric acid was added to the mine waters to neutralize their pH. The conspicuous occurrence of an otherwise extremely rare (known only from very few localities, such as Ivigtut, SW Greenland; Bailey 1980) association of Ba-Ca fluorides including zharchikite (Fig. 6), usovite, prosopite, and gearksutite is certainly related to this massive introduction of fluoride (assemblage SS3b, table 3).

Discussion

Hydrothermal mineral associations

Age. It is obvious from the above list of primary hydrothermal mineral associations that the Clara vein

←

Fig. 4. (continued) gangue was found on the mine floor next to a decomposing piece of pyrite-marcasite-chalcopyrite. Langite/posnjakite crusts formed within weeks. 7 cm. (e) and (f) Native copper and cuprite octahedra are associated with black delafossite aggregates on brownish goethite pseudomorphing siderite. 4 and 3 mm. (g) Native copper and cuprite on a goethite crust. 5 mm.

Downloaded from https://pubs.geoscienceworld.org/canmin/article-pdf/57/4/427/4800215/i1499-1276-57-4-427.pdf
by University of Arizona user

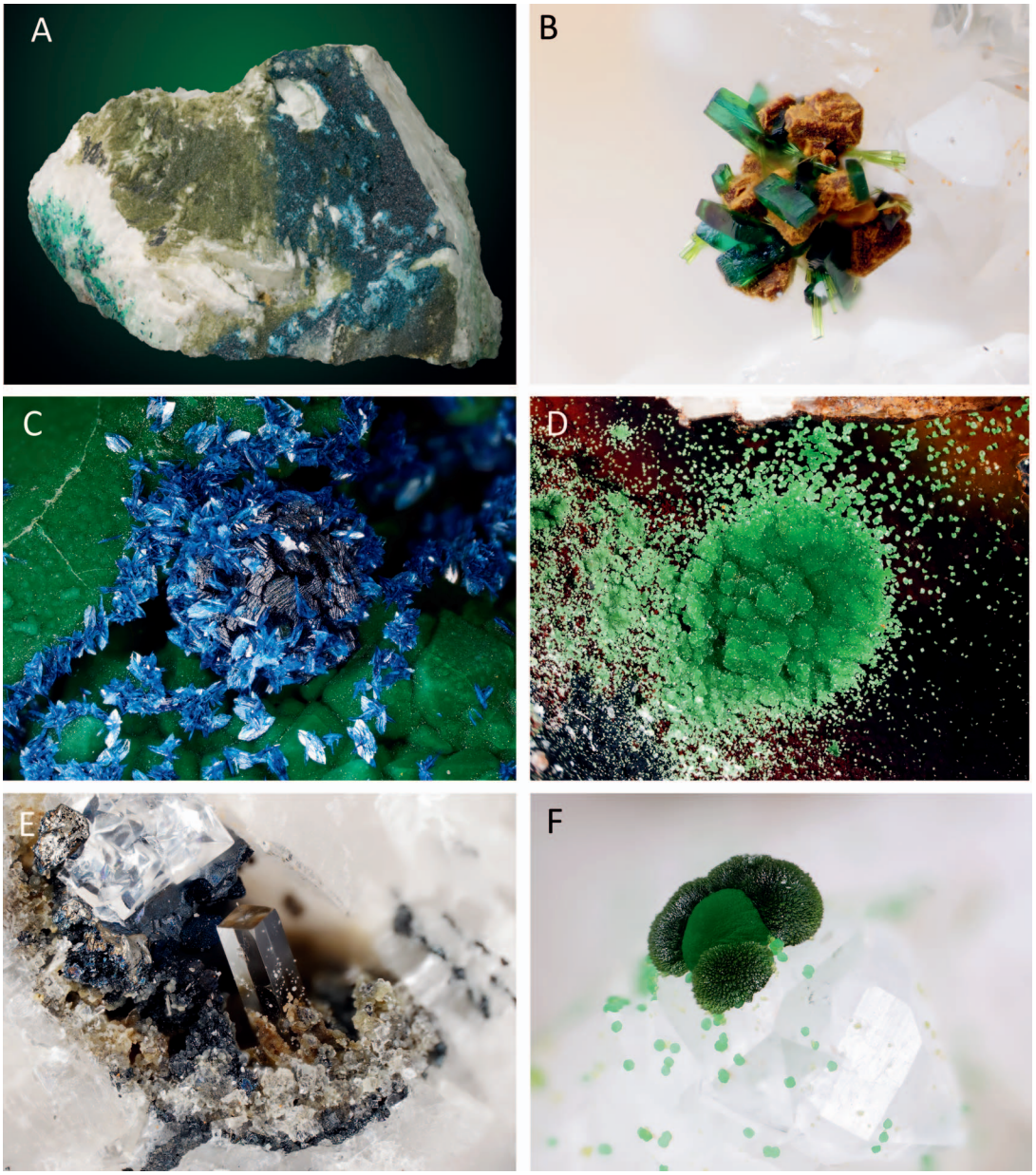

FIG. 5. Various typical mineral associations of the Clara deposit as discussed in the text. (a) Three copper arsenates on one specimen in a nice spatial arrangement: cornwallite (left side) fracture coating, olivenite (central part), and clinoclase (right side). 10 cm. (b) Cornwallite crystals with some agardite needles on goethite pseudomorphing chalcopyrite. 3 mm. (c) Azurite crystals overgrowing a clinoclase ball which itself grew on a crust of cornwallite (dark green). 7 mm. (d) Bayldonite crystals on goethite. 1 cm. (e) Anglesite crystal with some anhedral cerussite and blueish covellite replacing a galena crystal. 5 mm. (f) Bayldonite (center) surrounded by darker green duftite crystal aggregates and by tiny cornwallite spherules. 3 mm.

Downloaded from https://pubs.geoscienceworld.org/canmin/article-pdf/57/4/427/4800215/i1499-1276-57-4-427.pdf
by University of Arizona user

system is unusually diverse with respect to its primary mineralogy. This primary diversity is a major reason for the immense diversity of (hydrothermal and supergene) secondary phases which has developed in the vein. The ages of the primary hydrothermal mineral associations range, as detailed above, from Jurassic for the silification phase (around 170 Ma) and the fluorite and baryte veins (145 to 130 Ma; Pfaff *et al*. 2009 and Mertz 1987) to Neogene for the carbonate-sulfate associations (40–0.6 Ma, Burisch *et al*. 2018, Walter *et al*. 2018b). It is important to emphasize that the development of mineral diversity is related to three factors: (1) the elemental variability in the various primary hydrothermal stages, (2) the superposition of these various hydrothermal fluid influxes, *i.e*., the overprint of an older by a younger hydrothermal stage with different fluid composition and temperature, and (3) supergene oxidation of the various primary assemblages. Most of the unusual variability of the sulfide phases is due to these hydrothermal recrystallization and remobilization processes. This is especially notable for the various Ag- and Bi-bearing sulfosalts related to later hydrothermal overprint of primary Ag-bearing "fahlore" (association P5a) and Bi-bearing galena (association P6), respectively.

The reason for the large variety of the hydrothermal assemblages lies, in the authors' view, in the chemical and thermal variability of the ore-forming fluids. All post-Permian veins in the Schwarzwald are interpreted to have formed due to mixing of a hot basement brine with various types of cooler, upper crustal fluids (*e.g*., Staude *et al*. 2009). These upper crustal fluids gained their chemical properties by reaction with their various aquifers, which included both quartzitic rocks and various types of limestone (*e.g*., Walter *et al*. 2018a and many of the references cited in the Introduction). Walter *et al*. (2018a, 2019) showed that mixing the basement brine with these various fluids produced quite variable hydrothermal assemblages upon precipitation. For example, Cu- and Ni-rich associations found close to the Rhinegraben in a number of veins are believed to reflect admixing of fluids from the Buntsandstein aquifer with the basement brine, while the more common Pb- and Zn-rich veins probably record the involvement of Muschelkalk fluids. It is, up to now, impossible to uniquely relate a specific mineral assemblage or association in a hydrothermal vein to a unique process involving a very specific fluid composition, but it is clear from our broader view of hundreds of Schwarzwald hydrothermal veins that the many pulses of obviously variable hydrothermal fluids entering the Clara vein system are responsible for the notable diversity of primary mineralization. All types of mineralization found within the Clara vein have been described from hydrothermal veins within a 20 km radius, but only the Clara vein system combines all of them in one deposit. Only here, hence, could hydrothermal superposition and supergene oxidation combine all of these elements to form the vast number of secondary minerals observed. Details of the conditions of formation for the baryte-"fahlore", the fluorite-sellaite, and the carbonate-gypsum associations can be found in Keim *et al*. (2018b), Pfaff *et al*. (2012), and Burisch *et al*. (2018), respectively.

The Scheelitmaterial. A particularly interesting type of rock is the Scheelitmaterial (association P2, Tables 1 and 2), which has never been previously mentioned in scientific reports on the Clara vein. This is surprising, as it accounts for a diverse and quite unusual set of minerals dominated by W and V phases. Scheelitmaterial can be easily recognized in hand specimen, as it consists in large part of a fine-grained, cherty, reddish-brown material (Fig. 4a) composed of silicified clay material rich in iron (hematite), probably formed in two stages: hydrothermal alteration of primary host rock minerals (biotite, plagioclase) to a hematite-clay mixture, which was deposited in the Clara vein system and which was silicified there in a second stage during a later hydrothermal event. The Fe-rich clay material was able to adsorb large-ion lithophile elements like W and V and was, thus, enriched in these elements. Upon silicification, these elements were remobilized and combined with elements from the silicifying fluid (*e.g*., Ca, Cu) to form W-V minerals such as ferberite, scheelite, and roscoelite. Later supergene overprint increased this variability by producing mineral phases such as rankachite, cuprotungstite, hydrotungstite, "ferritungstite" (= hydrokenoelsmoreite), phyllotungstite, and others which form crystal aggregates in vugs lined with quartz crystals and in fractures (Fig. 4b).

Primary zoning in the baryte vein. Finally, it is important to emphasize that primary hydrothermal associations P4, P5a, and P5b all come from the baryte vein. Importantly, the northern part of the baryte vein (Nordfeld, Table 1) contains much less (if any) "fahlore" than the southern part (Südfeld, Table 1), where this mineral group is mined as Ag ore (Silberspat, Table 1). This has an important bearing on secondary mineralogy, as will be discussed in the next section on supergene mineral associations. In addition, the interplay between Fe-dominated sulfides (pyrite, marcasite, with some chalcopyrite) and Cu-dominated sulfides ("fahlore" with chalcopyrite) in the baryte vein sets the stage for the variability of the later supergene assemblages and associations.

Downloaded from https://pubs.geoscienceworld.org/canmin/article-pdf/57/4/427/4800215/i1499-1276-57-4-427.pdf
by University of Arizona user

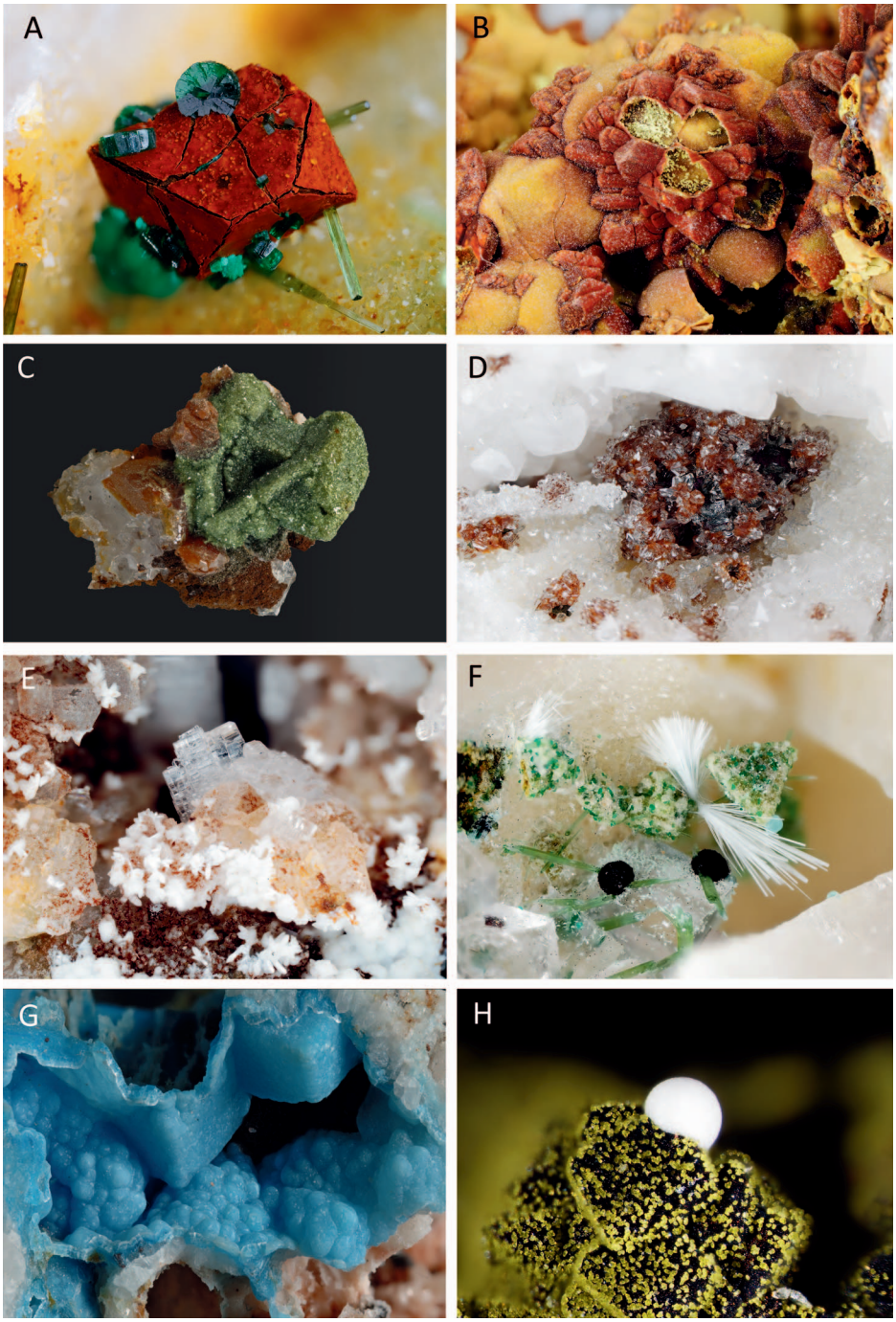

FIG. 6. Various typical mineral associations of the Clara deposit as discussed in the text. (a) Cornwallite "wheels" with agardite needles on goethite replacing chalcopyrite. 4 mm. (b) Reddish and orange-brown bariopharmacosiderite overgrowing and replacing scorodite crystals (hollow). 7 mm. (c) Green bariopharmacosiderite crystals overgrowing large chalcopyrite crystals. 3 cm. (d) Colorless, sparkling scorodite crystals overgrowing goethitized chalcopyrite. 5 mm. (e) The rare fluoride mineral zharchikite overgrowing third-generation baryte as the youngest phase—it probably formed due to anthropogenic

Downloaded from https://pubs.geoscienceworld.org/canmin/article-pdf/57/4/427/4800215/i1499-1276-57-4-427.pdf
by University of Arizona user

Supergene mineral associations

Age. Burisch *et al*. (2018) dated and modelled the erosional uplift of some Schwarzwald mineral veins (including the Clara vein) based on the conspicuous occurrence of primary association P8 (Table 2). According to this work, uplift and erosion started around 20 Ma and the last hydrothermal fluids entered the veins at approximately 0.6 Ma. The first truly supergene mineral assemblages (Fe and Mn oxides) were dated by Hautmann & Lippolt (2000) to about 15 Ma and oxidative modification of the hydrothermal mineral assemblages in the Schwarzwald veins continues today.

Some of the supergene assemblages, such as the copper sulfates (langite, brochantite) on marcasite and chalcopyrite, can form within weeks (as observed by miners on fresh ore specimens lying on the floor of the mine; see *e.g*., Fig. 4D).

Large-scale zoning. Upon entering the vein system, meteoric fluids are in disequilibrium with all gangue and ore minerals. As they could enter the openly outcropping vein through fractures and did not have to percolate through soil, they are oxygen-rich (in equilibrium with the atmosphere) and solute-poor. Based on our textural observations detailed above, they dissolved baryte, fluorite, quartz, carbonates, and the ore minerals and developed a reducing character or retained their oxidizing character depending on the gangue/sulfide ratio during fluid/rock interaction (dissolution of baryte or fluorite does not have any influence on redox conditions in the fluid). The formation of the famous secondary baryte crystals (Meißelspat, Table 1, see Fig. 3) or of young fluorite crystals on botryoidal Fe-hydroxide aggregates (Fig. 3) shows that these phases were only redistributed within the vein – at distances on the orders of centimeters, meters, or hundreds of meters. Loges *et al*. (2012a) showed (based on Ce-anomaly studies in secondary Mn-minerals formed during the decomposition of Mn-bearing carbonates like siderite) that the supergene fluid composition may change within millimeters and that the whole water-saturated vein consists of many millions of micro-compartments which all have their own composition and physicochemical conditions (redox and pH being the most important ones).

Redox conditions in the deeper parts of the mine are probably controlled by Fe^{2+}/Fe^{3+} and by sulfate/sulfide equilibria. While Fe^{3+}-minerals, especially botryoidal goethite, are common in the upper parts of the mine (gossan), they become rarer with increasing depth. The vein, hence, shows the classical zoning from sulfide-free, goethite-rich upper parts to pristine ore at depth. Interestingly, however, there is no clearly observable zone of reduction with native copper or silver which would be linked to the water table, as in the classical examples such as the White Pine copper deposit, Michigan (Brown 1971); Santa Rita ore district, New Mexico; Naukat, Central Asia (Cornwall 1956 and references therein); or the Cerro Maimón VMS deposit, Dominican Republic (Andreu *et al*. 2015), just to name a few. Rather, pristine oxidized and reduced assemblages occur in the above-mentioned micro-compartments at many levels. This may be a consequence of artificial changes of the water table by the active mine over decades, or it may be a specific feature of the Clara vein due to inhomogeneous dissolution in the large and mineralogically diverse vein system.

It should also be mentioned that the temperature changes quite significantly from the surface (about 10 °C average annual temperature; Deutscher Wetterdienst 2012) to depth (almost 30 °C at the deepest mine level today, Kovac, *pers. commun*.). This temperature difference may exert a significant control on supergene mineral stability (see *e.g*., Haßler *et al*. 2014).

Source of elements. The elements available for the formation of secondary phases at a specific place in the vein system consist of locally derived elements and of elements transported from further away by the supergene fluid. This depends on the mobility of the various elements. Iron-bearing minerals tend to form in close vicinity (*i.e*., within millimeters) or even as pseudomorphs after primary sulfides. Typical examples include scorodite-bariopharmacosiderite-dussertite assemblages on or around altered chalcopyrite (Fig. 6). Likely depending on pH and/or redox specifics, these assemblages occur with or without goethite. Here, arsenate and Ba were mobile, Fe immobile. Cornwallite and agardite overgrowing goethite pseudomorphs after chalcopyrite (Fig. 6) prove arsenate and REE mobility and Fe and Cu

←

FIG. 6. (continued) input of HF into the mine. 6 mm. (f) White needles of ettringite and black tenorite pseudomorphing malachite spherules and indicating that high-pH fluids containing Ca formed this supergene association, most probably due to anthropogenic input of concrete into the mine. Note that green cornwallite (spherules) and olivenite (needles) are older supergene phases not altered by the high-pH-Ca association. 8 mm. (g) Blue crusts of arsenogorceixite record Al mobility; this is probably also an effect of the high-pH fluids due to concrete addition. 1 cm. (h) Crandallite is a younger phase than dussertite, and this is typical; the phases recording Al mobility (such as crandallite-group minerals) are always younger than any other supergene minerals, again supporting the involvement of concrete in their formation. 4 mm.

Downloaded from https://pubs.geoscienceworld.org/canmin/article-pdf/57/4/427/4800215/i1499-1276-57-4-427.pdf
by University of Arizona user

immobility. The REE may be derived from either the country rocks or from the dissolution of REE-bearing fluorite (see Göb *et al*. 2011). The occurrence of Pb-bearing phases such as beudantite/segnitite or of U-bearing phases like zeunerite/torbernite in the "fahlore"-dominated parts of the baryte vein shows that Pb and U were transported over relatively large distances (probably tens to hundreds of meters) from the Diagonaltrum and the Fluoritgang (Table 1), respectively, into the baryte vein. The restriction of supergene Bi, Co, and Ni phases to close proximity to their primary ores (Bi-bearing galena, "fahlore", and gersdorffite, respectively) is probably not related to their immobility (as these elements are typically very mobile in supergene environments, *e.g*., Markl *et al*. 2014), but to their dilution while being transported over greater distances. Copper, Pb, and Fe are much more common than those elements, so they do not form their own phases far away from the site of mobilization. In this respect, it is interesting to note that Zn minerals clearly become rarer with depth. As "fahlore" is the main source of Zn in the vein (sphalerite being exceptionally rare and confined to some late carbonate veinlets), this observation could be explained by a higher Zn content in "fahlore" at shallow depths, although this was not observed in the study of Keim *et al*. (2018b). Therefore, the rarity of Zn minerals at depth is interpreted to reflect a temperature effect (the 10 to 30 °C change mentioned above).

The restriction of a conspicuous association of iron phosphates to the northern part of the baryte vein (Nordfeld, Table 1) and the lack of primary phosphates in the Clara vein system indicates (1) the addition of phosphate from the country rocks, and (2) the restricted lateral mobility of arsenate in the baryte vein. As the phosphate content of the supergene fluid is probably buffered by apatite in the host rocks, it should be similar in all parts of the mine, but the phosphate/arsenate ratio in the supergene fluids most likely changes with increasing distance from the "fahlore"-rich parts of the baryte vein (which are in the south; see above). Iron phosphate minerals are apparently only stable far away (tens to hundreds of meters) from the "fahlore", *i.e*., in equilibrium with fluids poor in arsenate.

Barium, Ca, and Sr present in many common supergene minerals like bariopharmacosiderite, dussertite, and crandallite-group minerals are most likely derived from the dissolution of the gangue minerals (note that Ca may also be derived from concrete and from plagioclase alteration in the host rocks). Also, the source of Cu and Fe for the amazing variety of supergene Cu and Fe minerals is easily related to weathered "fahlore" and chalcopyrite. Secondary Sb minerals like tripuhyite, cervantite, and cualstibite are also clearly related to weathered "fahlore" or other Sb-bearing sulfosalt minerals, such as pyrargyrite and polybasite. Secondary W minerals do not only occur in the Scheelitmaterial, but also, *e.g*., in the Silberspat (Table 1), where tungstibite or raspite were locally common supergene phases, and in the Diagonaltrum (Table 1), where stolzite is a common supergene Pb mineral. The W in a phase such as stolzite could be derived from either the Scheelitmaterial or the country rocks, as is the case for W-rich goethite at the nearby Hohberg locality, St. Roman (Markl 2016), and at the nearby Fortuna mine, Gelbach, near Wolfach (Markl 2017). Which possibility is correct remains unclear.

In summary, supergene phases in the alteration micro-compartments in the Clara vein system form from elements locally available (Fe, Cu, Sb, Bi, Co, Ni), from elements transported from dissolved parts of the vein to the site of mineral formation (Ca, Ba, Sr, Pb, As), and from elements derived from host rock alteration (phosphate, REE, some Ca, possibly W).

Anthropogenic mineral associations

Anthropogenic effects are, in summary, the introduction of Ca and F and significant pH changes at certain times and in certain parts of the deposit. While the addition of Ca and F can be relatively easily related to certain newly formed mineral associations (ettringite, tenorite pseudomorphic after malachite, calcite, Ca arsenates and various fluorides; see above), the pH increase may have a much broader impact than seen at first glance. Keim *et al*. (2017), Markl (1998), and Kolitsch (1997) suggested that certain "naturally looking" mineral assemblages like the ones with clinoclase in the "fahlore"-bearing baryte vein or the hydrocerussite-litharge-elyite assemblage from the Diagonaltrum would not have formed under completely natural conditions, but were only made possible by the anthropogenic pH increase.

Lastly, the unusually common occurrence of Al-bearing supergene phases of the crandallite group (such as gorceixite, goyazite, and crandallite and their respective arsenate endmembers; Fig. 6) implies unusual Al mobility in the supergene fluids (supergene fluids sampled in the Clara mine have up to 0.04 mg/l Al; Göb *et al*. 2013, Loges *et al*. 2012a, Bucher *et al*. 2009). As such, an Al mobility is only realized in either very acid or very basic pH fluids; as the non-anthropogenic supergene fluids are host-rock buffered and, hence, more or less neutral, the crandallite-group minerals may also form as a consequence of anthropogenic pH increase.

Downloaded from https://pubs.geoscienceworld.org/canmin/article-pdf/57/4/427/4800215/i1499-1276-57-4-427.pdf
by University of Arizona user

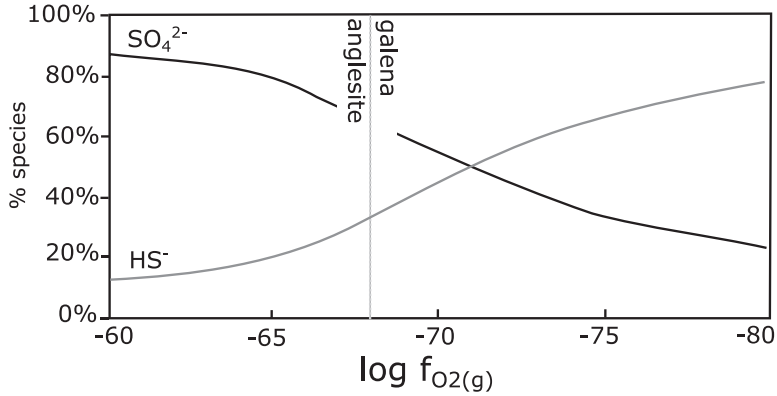

FIG. 7. The stability of galena and anglesite related to the relative importance of HS^- and SO_4^{2-} at variable log f_{O_2} conditions at 25 °C and 1 bar. The dashed line shows the predominance boundary of anglesite and galena.

Fluid chemistry of the Clara Mine and model setup

Fluids sampled in and in the vicinity of the Clara mine (dripping water, borehole water, rainwater, snow, and surface water) were analyzed by Göb *et al*. (2013), Loges *et al*. (2012a), and Bucher *et al*. (2009). These fluids show pH between 4.82 and 9.6 and temperatures between 5 and 22.7 °C. All waters are Ca-Na-SO_4^{2+}-HCO_3^--dominated and are close to equilibrium with the atmosphere regarding oxygen (approximate log f_{O_2} of –0.68). Besides main cations and anions, Göb *et al*. (2013) also reported concentrations of Cu, Fe, Co, Pb, Mn, Cr, Bi, Sb, As, and Ni, while Loges *et al*. (2012a) analyzed the REE contents.

Based on these literature values, we chose realistic ion activities as input parameters for the stability diagrams presented below. The specific input parameters for each predominance diagram are given in the figure captions. For the fluid path models, a rainwater analysis from Bucher *et al*. (2009) was selected (Fluid A: Na 0.1 mg/l; K = 0.1 mg/l; Ca = 0.4 mg/l; Cl = 0.3 mg/l; S = 0.4 mg/l), and the starting pH was set to different values (5.8, 7.5, 8.5). The temperature was set to 25 °C for all calculations.

Hydrogeochemical modelling

The Geochemist's Workbench version 10.0 was used for calculating phase predominance diagrams, and phase stability diagrams were calculated using version 12.0 of the same program (Bethke & Yeakel 2015). Fluid path modelling was done using Phreeqc version 2.18.3 (Parkhurst & Appelo 1999). All calculations are based on the Thermoddem data base (Blanc *et al*. 2012). Data for duftite, conichalcite, cornubite, and bayldonite were added from Magalhaes *et al*. (1988) and for leadhillite, caledonite, and linarite from Abdul-Samad *et al*. (1982). The consequences of such data base additions are discussed in Keim *et al*. (2017).

Figures 7 to 14 show various stability diagrams and the results of reaction-path modeling pertinent to some of the most conspicuous assemblages in the Clara vein system. The diagrams help to understand the complex evolution of the supergene fluids in the compartmentalized vein system during meteoric water influx, and they also illustrate that small changes in starting fluid composition or in mass fractions of minerals involved in dissolution or precipitation reactions can change the resulting assemblages significantly. The figures quantify some of the processes responsible for the large diversity of mineral assemblages in the Clara deposit; further quantifications for both hydrothermal and supergene processes are found in Pfaff *et al*. (2012; hydrothermal formation of the sellaite-fluorite vein system), Keim & Markl (2015; reaction-path modelling and phase stabilities during weathering of galena), Keim *et al*. (2016; silver redistribution during weathering of galena), Keim *et al*. (2017; formation of basic lead phases due to the influence of concrete), Keim *et al*. (2018b; formation and zoning of the Silberspat in the Clara deposit, Table 1), and Burisch *et al*. (2018; formation of the carbonate-gypsum association). Together, these works and the new calculations illustrate the diversity of the conditions of formation of the various typical assemblages in the Clara vein system, and this is the basis on which the stunning mineralogical diversity formed.

Figure 7 shows the influence of redox conditions on galena stability. Some hand specimens show apparently stable galena-anglesite assemblages which constrain (at fixed *P*, *T*, and pH) the redox conditions of the participating fluid. At 25 °C, this would be a log f_{O_2} of about 10^{-68} (Fig. 7). Figure 8 shows the influence of

Downloaded from https://pubs.geoscienceworld.org/canmin/article-pdf/57/4/427/4800215/i1499-1276-57-4-427.pdf
by University of Arizona user

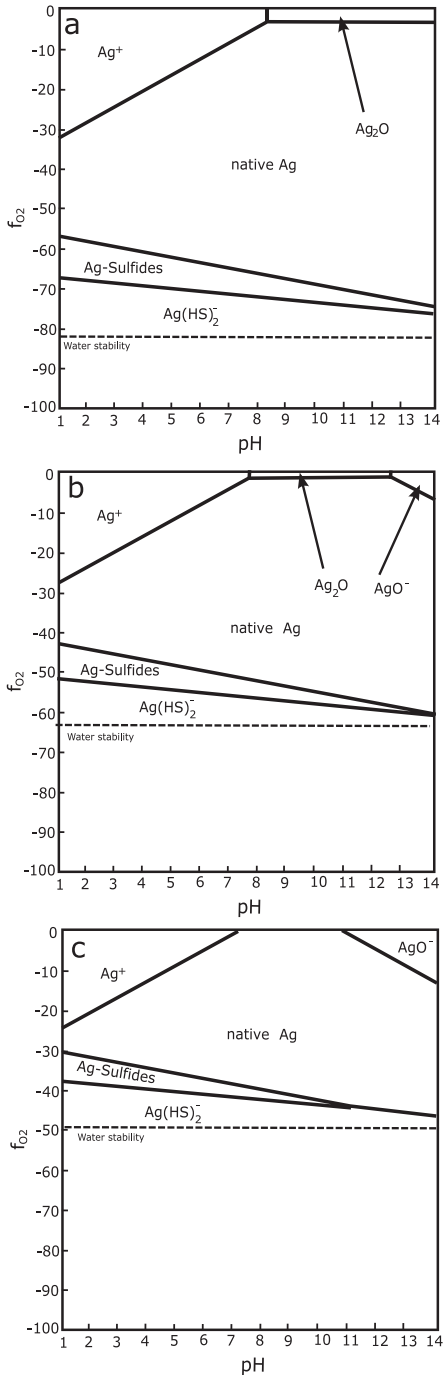

FIG. 8. Stability of native silver and acanthite in supergene environments (see also Fig. 2): (a–c) f_{O2}-pH phase predominance diagram for native silver, aqueous Ag-species, and Ag-sulfides for temperatures of 25, 100, and 250 °C. Input parameters: $\log a_{Ag+} = -3$; $\log a_{SO42-} = -3$; Ag^+ as the main species.

temperature on the stability relations of hypo- to supergene silver phases (acanthite/argentite and native silver, which are the most common ones). With increasing temperature, the stability field of native silver decreases and is shifted to higher oxygen fugacities (which, however, does not say anything about the relative redox conditions due to the temperature dependence of oxygen fugacity buffers). Interestingly, the stability field of native silver is always much larger than those of the silver sulfides. The stability relations amongst the Fe and Cu sulfates are shown in Figure 9. Whereas jarosite is a phase observed in supergene assemblages together with, *e.g.*, brochantite and antlerite, melanterite was never observed as a natural phase, but only formed on collected specimens (as was chalcanthite). It is obvious that pH exerts the main control on these phase stabilities and that the copper-bearing species require higher pH conditions than the iron-bearing ones. In the actual oxidation process in the mine, this probably relates to the gangue/ore mass ratio in a specific portion of weathered vein, to the presence of carbonates increasing the pH during weathering, and to fluid interaction with concrete. Only the last of these would explain the langite/posnjakite crusts shown in Figure 4D, which develop within weeks in the mine, as only the reaction with concrete would buffer pH at values significantly above neutrality. Samples thickly covered by antlerite indicate the same process and, hence, the nice copper sulfate specimens from the Clara mine are most probably only "semi-natural".

The interesting assemblage of delafossite with cuprite, native copper, and, in rare cases, native silver develops in the vicinity of weathering siderite crystals (see Fig. 4). An oxidized copper- and silver-bearing fluid percolated through the vuggy vein and reacted at certain places with siderite. At appropriate pH conditions (see Fig. 10), the sequence of delafossite, cuprite, and native metals formed during continuous reduction of the reacting fluid. The formation of goethite shows that reduction of Cu and Ag is caused by oxidation of Fe^{2+} to Fe^{3+}.

The formation of the famous copper and copper-lead arsenates, such as clinoclase, olivenite, cornwallite, duftite, bayldonite, and mimetite, was intensively investigated by Magalhaes *et al.* (1988). This work presents a series of diagrams to explain the conditions of formation of the various arsenate assemblages. Figure 11 shows a diagram newly calculated so as to be pertinent to what exactly is observed in the Clara vein system. Obviously, the pure copper arsenates are only found at very low Pb activities in the supergene fluid (below 10^{-7}), and their stability among each other depends solely on pH. Hence, a specimen such as the one shown in Figure 5a, where olivenite, cornwallite,

Downloaded from https://pubs.geoscienceworld.org/canmin/article-pdf/57/4/427/4800215/i1499-1276-57-4-427.pdf
by University of Arizona user

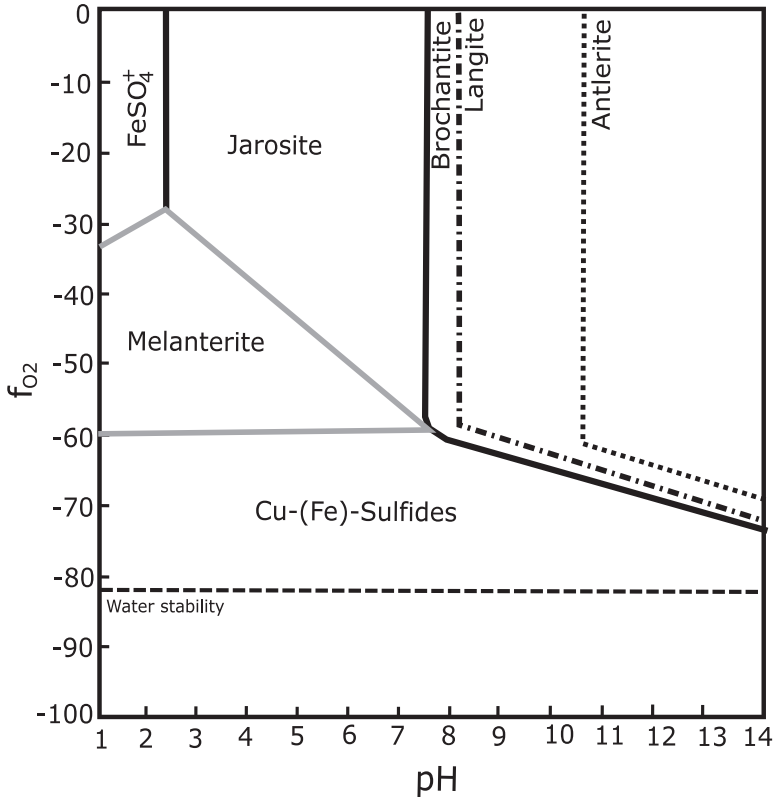

FIG. 9. Stability relations among Fe-Cu sulfates (see also Fig. 4): f_{O2}-pH phase predominance diagram for jarosite, melanterite, Cu-Fe sulfides (overlapping stability of chalcocite, bornite, and covellite), brochantite, langite, and antlerite calculated with sulfate as the main species. Input parameters: $T = 25$ °C; $\log a_{Fe3+} = -3$; $\log a_{Cu2+} = -4$. The dashed boundaries show that the mineral predominance fields (langite and antlerite) are concealed by brochantite and only appear when the latter is suppressed. Note that schwertmanite was suppressed because of its large, overlapping predominance field. Melanterite stability was attained only at water activities >1 and is therefore extrapolated down to a water activity of 1.

and clinoclase are present within centimeters of each other and in a clear, spatial arrangement, records pH changes on the centimeter scale during mineral precipitation. At higher Pb activities, a diverse suite of Pb- and Pb-Cu-arsenates form. Interestingly, their stability is mainly dependent on the Pb/Cu ratio (Fig. 11).

As described above, the baryte vein shows two different facies: a "fahlore"-rich facies in the south ("silver spar") and a "fahlore"-poor (or even "fahlore"-free) facies in the north. Both facies contain small amounts of chalcopyrite. In the north, goethite together with an interesting suite of Fe, Cu, and Sr-bearing phosphates forms the supergene assemblages, and the "silver spar" shows typical arsenate assemblages such as the ones shown in Figures 5 and 6a. This is obviously related to the phosphate/arsenate ratio in the supergene fluid, and Figure 12 quantifies this using the example pair scorodite-strengite. This figure also shows that soil and mine water analyses are exactly in the range which allows small variations of arsenate or phosphate in the fluid to determine the stability of the Fe phosphate or the Fe arsenate. Interestingly, host-rock buffered fluids would almost invariably crystallize the phosphate strengite, while meteoric fluids which have reacted with soil contain less phosphate and, hence, would stabilize Fe arsenates. However, the amount of (As-rich) "fahlore" in the whole deposit is so large that scorodite rather than strengite is the more common phase.

The effect of concrete on the mine waters has been discussed above and (for Pb-bearing phases) in the work of Keim *et al*. (2017). It is instructive to take a closer look at Cu-bearing associations, as they show an interesting reaction texture. Upon reaction of a Ca-rich, high-pH fluid (in equilibrium with concrete) with

Downloaded from https://pubs.geoscienceworld.org/canmin/article-pdf/57/4/427/4800215/i1499-1276-57-4-427.pdf
by University of Arizona user

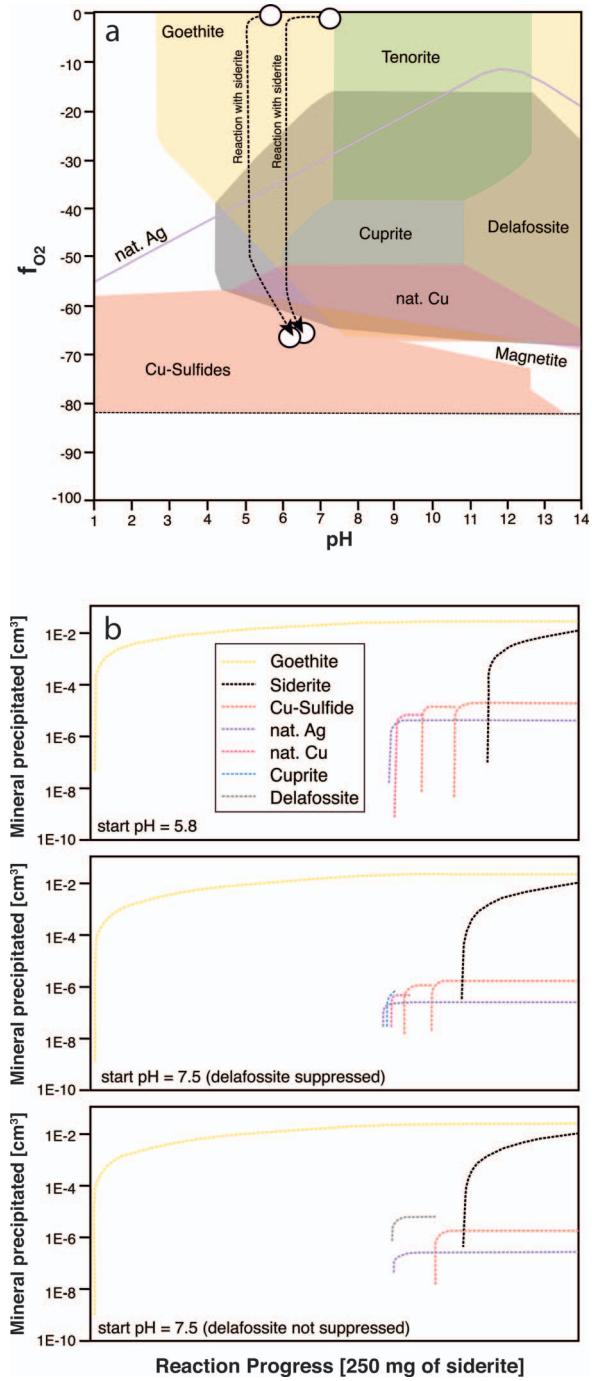

FIG. 10. Reaction-path modeling to understand the formation of the delafossite-cuprite-native copper assemblages in the vicinity of corroded siderite (see Fig. 4). (a) f_{O2}-pH phase stability diagram for goethite (yellow), magnetite (white), tenorite (green), cuprite (light grey), natural Cu (pink), natural Ag (purple), delafossite (grey field), and Cu-sulfides (red). Note that the stability fields are overlapping. Input parameters: $T = 25$ °C; $Fe^{3+} = -150$ µg/l; $Cu^{2+} = 75$ µg/l; $SO_4^{2-} = 100$ mg/l; $Ag^{+} = 10$ µg/l; $HCO_3^{-} = 100$ mg/l. Note that the diagram is calculated with delafossite suppressed and unsuppressed (grey field) because of its large stability field. The reaction path for "fluid A" (see text) reacting with 250 mg of siderite, for two

Downloaded from https://pubs.geoscienceworld.org/canmin/article-pdf/57/4/427/4800215/i1499-1276-57-4-427.pdf
by University of Arizona user

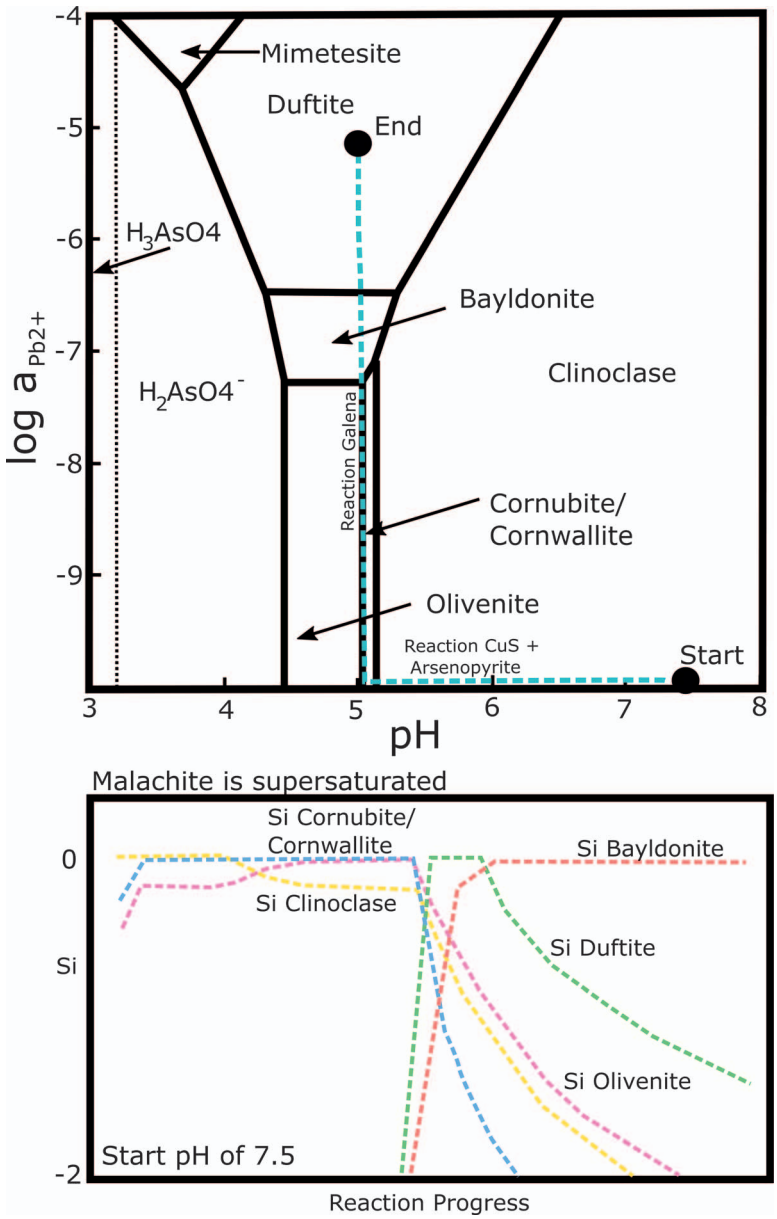

FIG. 11. Stability relations in the Cu-Pb-arsenate system to explain assemblages such as the ones shown in Figure 5. Loga_{Pb2+}-pH phase predominance diagram for mimetesite, duftite, bayldonite, olivenite, cornubite, and clinoclase calculated with arsenate as the main species. Input parameters: $T = 25$ °C; log$a_{H2ASO4-} = -6$; log$a_{Cu2+} = -2.5$; log$a_{Cl-} = -3$. Light blue lines show the calculated reaction path for "fluid A" (see text) reacting in 15 steps with 80 mmol of covellite followed by reaction with 0.1 mmol galena. Prior to the fluid path calculations, "fluid A" was equilibrated with 0.1 mmol arsenopyrite and covellite. This reaction simulates the reaction of a fluid with "fahlore" (arsenopyrite + covellite). The progressive saturation indices during the 15 reaction steps are shown in the lower part of the figure.

←

FIG. 10. (continued) different starting pH values of 5.8 and 7.5, is shown as black lines with arrows. (b) This diagram shows the progressive mineral precipitation in cm^3 during siderite reaction for the different pH values. Note that for pH = 7.5, the progressive mineral precipitation is calculated with delafossite suppressed (bottom) and unsuppressed (middle).

Downloaded from https://pubs.geoscienceworld.org/canmin/article-pdf/57/4/427/4800215/i1499-1276-57-4-427.pdf
by University of Arizona user

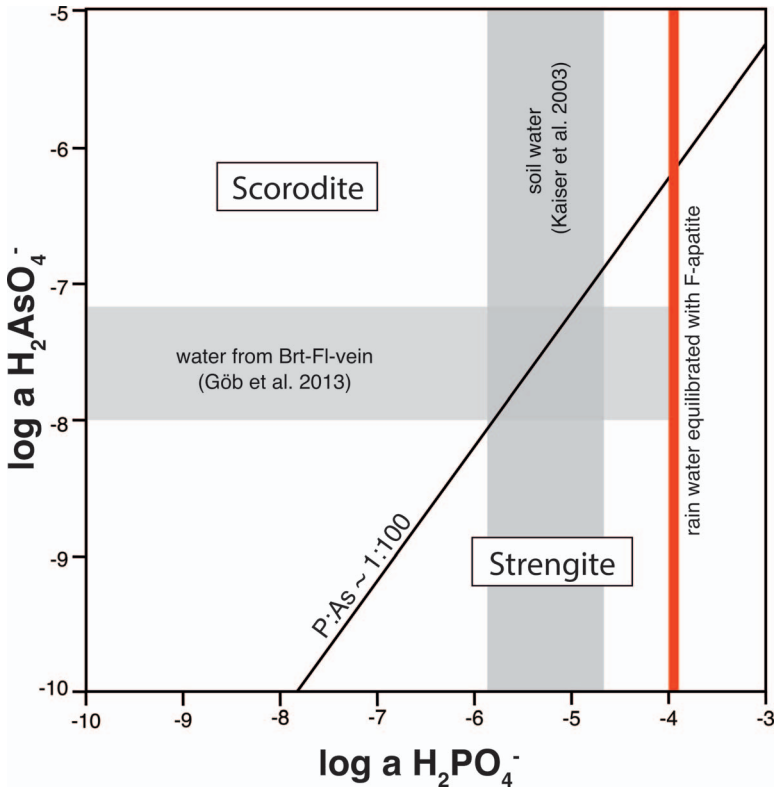

FIG. 12. Diagram illustrating the difference in fluid composition between the northern and the southern part of the baryte vein (Nordfeld & Südfeld, Table 1): $\log a_{H2AsO4}$-$\log a_{H2PO4-}$ phase predominance diagram for scorodite and strengite calculated with Fe as the main species. Input parameters: $T = 25$ °C; pH = 7; $\log a_{Fe3+} = -2$. The grey boxes show the $H_2AsO_4^-$ activity range for the Clara water analyses from Göb *et al*. (2013) and the soil water $H_2PO_4^-$ range from Kaiser *et al*. (2003). The red line marks the equilibrium concentration of $H_2PO_4^-$ in contact with fluorapatite (a common phase in the gneissic host rocks).

a supergene assemblage of, *e.g.*, malachite + olivenite + cornwallite, malachite will be converted to tenorite, while olivenite and cornwallite remain unaltered (see Fig. 6F). This alteration frees CO_2 and changes the pH of the fluid. As a consequence, ettringite and sometimes calcite precipitate as the youngest phases. The calculated fluid path in Figure 13 models the progressive reaction with concrete and shows that a malachite-brochantite assemblage stable at a more or less neutral pH is replaced by a tenorite-ettringite assemblage at pH values up to 12.

Supergene oxidation in the galena- and chalcopyrite-bearing Diagonaltrum leads to a large variety of assemblages or mineral successions. These involve both carbonates and sulfates of Cu and Pb. The various diagrams of Figure 14 illustrate how the various compositional variables (Cu, Pb, sulfate, carbonate activities, pH) contribute to this diversity of textures, successions, and assemblages. Again, it is obvious that small-scale processes operating during mineral dissolution and reprecipitation in a drusy vein can easily account for this diversity of observations.

SUMMARY AND CONCLUSIONS

Mineral diversity in the Clara hydrothermal vein type deposit, Schwarzwald, SW Germany, developed by a combination of: (1) the deposit being situated on or next to a large, crustal-scale, long-lived fault zone providing enhanced pathways for hydrothermal fluids; (2) many different hydrothermal fluid pulses transporting different suites of elements and, hence, producing different mineral assemblages and associations over at least the last 170 Ma; (3) hydrothermal modification of earlier mineral assemblages by later (multiple) fluid pulses; (4) supergene oxidation of the various primary ore assemblages during uplift and erosion of the deposit over the last few millions of

Downloaded from https://pubs.geoscienceworld.org/canmin/article-pdf/57/4/427/4800215/i1499-1276-57-4-427.pdf
by University of Arizona user

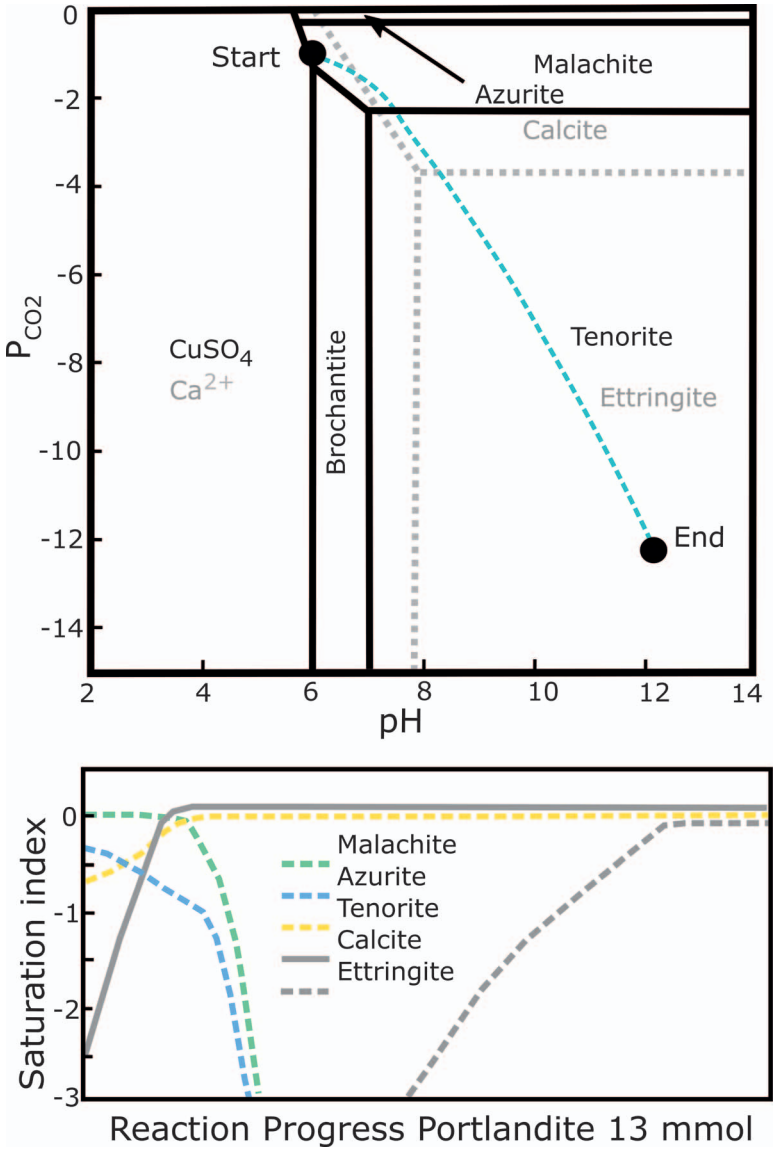

FIG. 13. Combined $\log P_{CO2}$-pH phase predominance diagram for brochantite, azurite, malachite, calcite, and ettringite for Cu^{2+} and Ca^{2+} as the main species. This diagram shows the effect of concrete addition on the supergene mineral assemblages. Most notably, the Ca sulfate ettringite (see Fig. 6) becomes a stable phase. Input parameters: $T = 25$ °C; $\log a_{Al3+} = -4$; $\log a_{SO42-} = -5$; $\log a_{Cu2+} = -3.5$. The light blue reaction path shows the progressive reaction of "fluid A" with 13 mmol of portlandite and 0.1 mmol of $Ca_2Al_2O_5 \cdot 8H_2O$. The latter was used to add alumina to the system, which is closed with respect to CO_2. The progressively changing saturation indices during the mineral reaction are shown in the lower part of the figure.

years; and (5) addition of artificial materials such as concrete, power plant ashes, and hydrofluoric acid to the mine, which reacted with the mine waters to produce a new assemblage of (partly) artificial minerals.

If the last of these points is estimated to be responsible for about 30–50 mineral species in the deposit, still more than 400 purely naturally formed minerals occur and render the Clara deposit one of the prime localities for mineral diversity on Earth. While

Downloaded from https://pubs.geoscienceworld.org/canmin/article-pdf/57/4/427/4800215/i1499-1276-57-4-427.pdf
by University of Arizona user

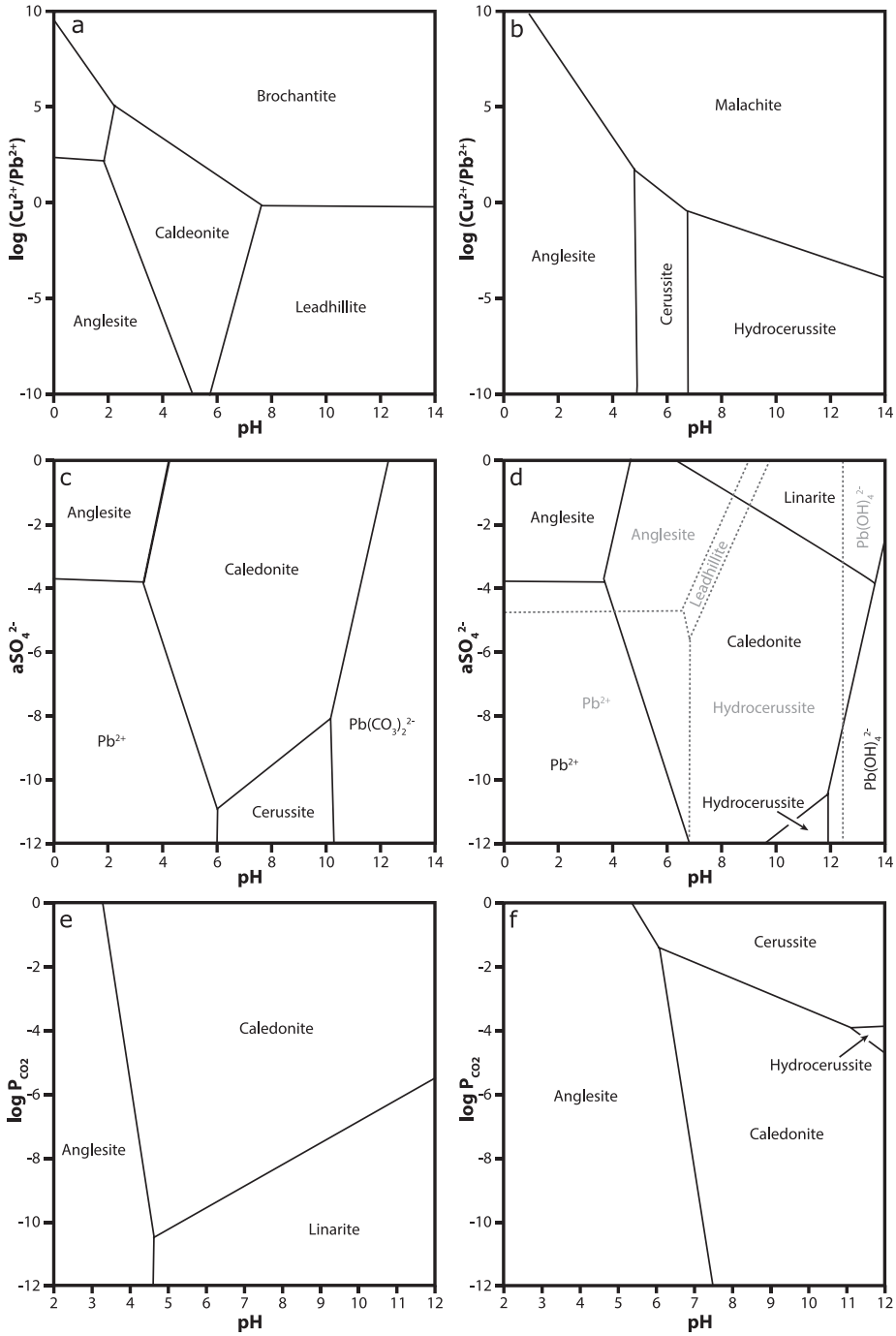

FIG. 14. Supergene mineral stabilities in the galena- and chalcopyrite-bearing Diagonaltrum (see Fig. 5). (a) Log(aCu^{2+}/Pb^{2+})-pH predominance diagram for the minerals brochantite, caledonite, anglesite, and leadhillite calculated with SO_4^{2-} as the main species. (b) Log(aCu^{2+}/Pb^{2+})-pH predominance diagram for malachite, hydrocerussite, and cerussite calculated with HCO_3^- as the main species. (c) Loga_{SO42-}-pH predominance diagram for caledonite, linarite, cerussite, and anglesite calculated with Pb^{2+} as the main species (log$a_{Pb2+} = -3$; $P_{CO2} = -3$; log$a_{Cu2+} = -5$). (d) Loga_{SO42-}-pH predominance

Downloaded from https://pubs.geoscienceworld.org/canmin/article-pdf/57/4/427/4800215/i1499-1276-57-4-427.pdf
by University of Arizona user

the hydrothermal processes typically affected large parts of the vein system in a similar manner (this notion is true despite some minor compositional depth zoning), supergene processes resulted in small-scale variations of fluid composition and may have, hence, produced different mineral assemblages on the scale of millimeters to centimeters. The combination of different hydrothermal associations to start with and these small-scale variations is the ultimate reason for the incredible wealth of mineral species to be found in this one deposit. The present contribution reports for the first time all hydrothermal "input" associations and models important supergene modifications of them. As all processes involved common upper-crustal basement regimes, it is very likely that similar combinations of hydrothermal and supergene processes exist at many places on Earth and, hence, that mineralogically diverse deposits are more common than presently believed or known. Only the artificial part involving concrete, ashes, and hydrofluoric acid may be unique to the Clara deposit.

Acknowledgments

We are grateful for financial support from the BMBF r[4] program ResErVar (project reference number 033R129E). Mineral photographs shown in Figures 2 to 6 were taken by Jeff Scovil (Fig. 3B–D), Wolfgang Gerber (Fig. 6C and G), Gregor Markl (Fig. 3A, 4A, and 5A), and Matthias Reinhardt (all others). Uwe Kolitsch, Wien, is thanked for information on the complete Clara mineral list and for help and support during the course of this study. We are very grateful for two thorough and constructive reviews by Simone Runyon and an anonymous reviewer, and for the perfect editorial handling by Matthew Steele-MacInnis.

References

Abdul-Samad, F., Thomas, J.H., Williams, P.A., Bideaux, R.A., & Symes, R.F. (1982) Mode of formation of some rare copper (II) and lead (II) minerals from aqueous solution, with particular reference to deposits at Tiger, Arizona. *Transition Metal Chemistry* **7(1)**, 32–37.

Andreu, E., Torró, L., Proenza, J.A., Domenech, C., García-Casco, A., de Benavent, C.V., & Lewis, J.F. (2015) Weathering profile of the Cerro de Maimón VMS deposit (Dominican Republic): Textures, mineralogy, gossan evolution and mobility of gold and silver. *Ore Geology Reviews* **65**, 165–179.

Bailey, J. (1980) Formation of cryolite and other alumino-fluorides : A petrological review. *Bulletin of the Geological Society of Denmark* **29**, 1–45.

Behr, H.J. & Gerler, J. (1987) Inclusions of sedimentary brines in post-Variscan mineralizations in the Federal Republic of Germany—A study by neutron activation analysis. *Chemical Geology* **61**, 65–77.

Behr, H.J., Horn, E.E., Frentzel-Beyme, K., & Reutel, C. (1987) Fluid inclusion characteristics of the Variscan and post-Variscan mineralizing fluids in the Federal Republic of Germany. *Chemical Geology* **61**, 273–285.

Bethke, C.M. & Yeakel, S. (2015) *GWB Essentials Guide*. Aqueous Solutions, LLC Champaign, Illinois, 149 pp.

Blanc, Ph., Lassin, A., & Piantone, P. (2012) Thermoddem: A geochemical database focused on low temperature water/rock interactions and waste materials. *Applied Geochemistry* **27**, 2107–2116.

Bliedtner, M. & Martin, M. (1986). *Erz- und Mineralla-gerstätten des Mittleren Schwarzwaldes*. Landesamt für Geologie, Rohstoffe und Bergbau (LGRB), Freiburg, Germany, 782 pp.

Bons, P.D., Fußwinkel, T., Gomez-Rivas, E., Markl, G., Wagner, T., & Walter, B. (2014) Fluid mixing from below in unconformity-related hydrothermal ore deposits. *Geology* **42**, 1035–1038.

Brown, A.C. (1971) Zoning in the White Pine copper deposit, Ontonagon County, Michigan. *Economic Geology* **66**, 543–573.

Bucher, K. & Stober, I. (2002) Water-rock reaction experiments with Black Forest gneiss and granite. *In* Water-Rock Interaction **40** (I. Stober & K. Bucher, eds.). Water Science and Technology Library book series, Springer, Dordrecht, Netherlands (61–95).

Bucher, K. & Stober, I. (2010) Fluids in the upper continental crust. *Geofluids* **10**, 241–253.

Bucher, K., Zhu, Y., & Stober, I. (2009) Groundwater in fractured crystalline rock, the Clara mine, Black Forest, Germany. *International Journal of Earth Sciences* **98**, 1727–1739.

Burisch, M., Walter, B.F., Wälle, M., & Markl, G. (2016a) Tracing fluid migration pathways in the root zone below unconformity-related hydrothermal veins: Insights from

←

Fig. 14. (continued) diagram for caledonite, linarite, cerussite, and anglesite calculated with Pb^{2+} as the main species ($\log a_{Pb2+} = -3$; $P_{CO2} = -7$; $\log a_{Cu2+} = -5$). (e) $\log P_{CO2-}$-pH predominance diagram for caledonite, linarite, and anglesite calculated with Pb^{2+} as the main species ($\log a_{Pb2+} = -3$; $\log a_{Cu2+} = -3$). (f) $\log P_{CO2-}$-pH predominance diagram for caledonite, linarite, hydrocerussite, and anglesite calculated with Pb^{2+} as the main species ($\log a_{Pb2+} = -3$; $\log a_{Cu2+} = -9$). All diagrams were calculated for 25 °C.

Downloaded from https://pubs.geoscienceworld.org/canmin/article-pdf/57/4/427/4800215/i1499-1276-57-4-427.pdf
by University of Arizona user

trace element systematics of individual fluid inclusions. *Chemical Geology* **429**, 44–50.

Burisch, M., Marks, M.A., Nowak, M., & Markl, G. (2016b) The effect of temperature and cataclastic deformation on the composition of upper crustal fluids—An experimental approach. *Chemical Geology* **433**, 24–35.

Burisch, M., Hartmann, A., Bach, W., Krolop, P., Krause, J., & Gutzmer, J. (2018) Genesis of hydrothermal silver-antimony-sulfide veins of the Bräunsdorf sector as part of the classic Freiberg silver mining district, Germany. *Mineralium Deposita* **54**, 263–280.

Burisch, M., Walter, B.F., Gerdes, A., Lanz, M., & Markl, G. (2018) Late-stage anhydrite-gypsum-siderite-dolomite-calcite assemblages record the transition from a deep to a shallow hydrothermal system in the Schwarzwald mining district, SW Germany. *Geochimica et Cosmochimica Acta* **223**, 259–278.

Burisch, M., Hartmann, A., Bach, W., Krolop, P., Krause, J., & Gutzmer, J. (2019) Genesis of hydrothermal silver-antimony-sulfide veins of the Bräunsdorf sector of the classic Freiberg silver mining district, Germany. *Mineralium Deposita* **2**, 263–280.

Cornwall, H.R. (1956) A summary of ideas on the origin of native copper deposits. *Economic Geology* **51**, 615–631.

Deutscher Wetterdienst (2012) *Mittelwerte der Temperatur bezogen auf den Standort 1961–1990*. Deutscher Wetterdienst, Offenbach, Germany.

Elsner, H. & Schmitz, M. (2017) Geofokus: Rohstoffgewinnung in Deutschland – Von tiefen Löchern und kleinen Flittern. *GMIT* **68**, 7–20.

Fußwinkel, T., Wagner, T., Wälle, M., Wenzel, T., Heinrich, C., & Markl, G. (2013) Fluid mixing forms basement-hosted Pb-Zn deposits: Insight from metal and halogen geochemistry of individual fluid inclusions. *Geology* **41**, 679–682.

Geyer, O.F. & Gwinner, M.P. (2011) *Geologie von Baden - Württemberg*. Schweizerbart'sche Verlagsbuchhandlung, Stuttgart, Germany, 627 pp.

Göb, S., Wenzel, T., Bau, M., Jacob, D.E., Loges, A., & Markl, G. (2011) The redistribution of rare-earth elements in secondary minerals of hydrothermal veins, Schwarzwald, southwestern Germany. *Canadian Mineralogist* **49(5)**, 1305–1333.

Göb, S., Loges, A., Nolde, N., Bau, M., Jacob, D.E., & Markl, G. (2013) Major and trace element compositions (including REE) of mineral, thermal, mine and surface waters in SW Germany and implications for water–rock interaction. *Applied Geochemistry* **33**, 127–152.

Haßler, K., Taubald, H., & Markl, G. (2014) Carbon and oxygen isotope composition of Pb-, Cu-and Bi-carbonates of the Schwarzwald mining district: Carbon sources, first data on bismutite and the discovery of an oxidation zone formed by ascending thermal water. *Geochimica et Cosmochimica Acta* **133**, 1–16.

Hautmann, S. & Lippolt, H.J. (2000) $^{40}Ar/^{39}Ar$ dating of central European K-Mn oxides – a chronological framework of supergene alteration processes during the Neogene. *Chemical Geology* **170**, 37–80.

Huck, K. (1984) *Beziehungen zwischen Tektonik und Paragenese unter Berücksichtigung geochemischer Kriterien in der Fluß- und Schwerspatlagerstätte "Clara" bei Oberwolfach/Schwarzwald*. Unpublished Ph.D. thesis, Universität Heidelberg, Germany 197 pp.

Ingwersen, G. (1990) *Die sekundären Mineralbildungen der Pb-Zn-Cu-Lagerstätte Tsumeb, Namibia (Physikalisch-chemische Modelle)*. Unpublished Ph.D. thesis, Universität Stuttgart, Germany, 233 pp.

Jamieson, H.E. (2011) Geochemistry and mineralogy of solid mine waste: essential knowledge for predicting environmental impact. *Elements* **7**, 381–386.

Kaiser, K., Guggenberger, G., & Haumaier, L (2003) Organic phosphorus in soil water under a European beech (Fagus sylvatica L.) stand in northeastern Bavaria, Germany: seasonal variability and changes with soil depth. *Biogeochemistry* **66**, 287–310.

Keim, M.F. & Markl, G. (2015) Weathering of galena: Mineralogical processes, hydrogeochemical fluid path modeling, and estimation of the growth rate of pyromorphite. *American Mineralogist* **100**, 1584–1594.

Keim, M.F., Vaudrin, R., & Markl, G. (2016) Redistribution of silver during supergene oxidation of argentiferous galena: A case study from the Schwarzwald, SW Germany. *Neues Jahrbuch für Mineralogie - Abhandlungen (Journal of Mineralogy and Geochemistry)* **193**, 295–309.

Keim, M.F., Gassmann, B., & Markl, G. (2017) Formation of basic lead phases during fire-setting and other natural and man-made processes. *American Mineralogist* **102**, 1482–1500.

Keim, M.F., Staude, S., Marquardt, K., Bachmann, K., Opitz, J., & Markl, G. (2018a) Weathering of Bi-bearing tennantite. *Chemical Geology* **499**, 1–25.

Keim, M.F., Walter, B.F., Neumann, U., Kreissl, S., Bayerl, R., & Markl, G. (2018b) Polyphase enrichment and redistribution processes in silver-rich mineral associations of the hydrothermal fluorite-barite-(Ag-Cu) Clara deposit, SW Germany. *Mineralium Deposita* **53**, 1–20.

Kolitsch, U. (1997) Eine durch Betoneinwirkung entstandene Paragenese von Blei-Verbindungen aus der Grube Clara im Mittleren Schwarzwald. *Der Erzgräber* **14**, 48–53.

Loges, A., Wagner, T., Barth, M., Bau, M., Göb, S., & Markl, G. (2012a) Negative Ce anomalies in Mn oxides: the role of Ce^{4+} mobility during water–mineral interaction. *Geochimica et Cosmochimica Acta* **86**, 296–317.

Downloaded from https://pubs.geoscienceworld.org/canmin/article-pdf/57/4/427/4800215/i1499-1276-57-4-427.pdf
by University of Arizona user

Loges, A., Wagner, T., Kirnbauer, T., Göb, S., Bau, M., Berner, Z., & Markl, G. (2012b) Source and origin of active and fossil thermal spring systems, northern Upper Rhine Graben, Germany. *Applied Geochemistry* **27(6)**, 1153–1169.

Magalhaes, M.C.F., De Jesus, J.D.P., & Williams, P.A. (1988) The chemistry of formation of some secondary arsenate minerals of Cu (II), Zn (II) and Pb (II). *Mineralogical Magazine* **52**, 679–690.

Markl, G. (1998) Kupferarsenat und -carbonatvergesellschaftungen aus der Grube Clara. *Der Erzgräber* **9**, 81–89.

Markl, G. (2015) *Schwarzwald, Lagerstätten und Mineralien aus vier Jahrhunderten; Band 1 Nordschwarzwald & Grube Clara*. Bode Verlag, Lauenstein, Germany, 665 pp.

Markl, G. (2016) *Schwarzwald, Lagerstätten und Mineralien aus vier Jahrhunderten; Band 2 Mittlerer Schwarzwald Teil 1*. Bode Verlag, Lauenstein, Germany, 648 pp.

Markl, G. (2017) *Schwarzwald, Lagerstätten und Mineralien aus vier Jahrhunderten; Band 3 Mittlerer Schwarzwald Teil 2*. Bode Verlag, Lauenstein, Germany, 640 pp.

Markl, G., Marks, M.A., Derrey, I., & Gühring, J.E. (2014) Weathering of cobalt arsenides: Natural assemblages and calculated stability relations among secondary Ca-Mg-Co arsenates and carbonates. *American Mineralogist* **99**, 44–56.

Mertz, D.F. (1987) *Isotopengeochemische und mineralogische Untersuchungen an postvariszischen hydrothermalen Silikaten*. Unpublished Ph.D. thesis, Universität Heidelberg, Germany, 156 pp.

Metz, R., Richter, M., & Schürrenberg, H. (1957) Die Blei-Zink Erzgänge des Schwarzwaldes. *Geologisches Jahrbuch: Beihefte* **29**, 1–277.

Parkhurst, D.L. & Appelo, C.A.J. (1999) *User's guide to Phreeqc (ver. 2)-A computer program for speciation, batch-reaction, one-dimensional transport, and inverse geochemical calculations*. United States Geological Survey Water-Resources Investigations Report 99-4259.

Pfaff, K., Romer, R.L., & Markl, G. (2009) U-Pb ages of ferberite, chalcedony, agate, "U-mica" and pitchblende: constraints on the mineralization history of the Schwarzwald ore district. *European Journal of Mineralogy* **21**, 817–836.

Pfaff, K., Hildebrandt, L.H., Leach, D.L., Jacob, D.E., & Markl, G. (2010) Formation of the Wiesloch Mississippi Valley-type Zn-Pb-Ag deposit in the extensional setting of the Upper Rhinegraben, SW Germany. *Mineralium Deposita* **45(7)**, 647–666.

Pfaff, K., Koenig, A., Wenzel, T., Ridley, I., Hildebrandt, L.H., Leach, D.L., & Markl, G. (2011) Trace and minor element variations and sulfur isotopes in crystalline and colloform ZnS: Incorporation mechanisms and implications for their genesis. *Chemical Geology* **286**, 118–134.

Pfaff, K., Staude, S., & Markl, G. (2012) On the origin of sellaite (MgF_2)-rich deposits in Mg-poor environments. *American Mineralogist* **97**, 1987–1997.

Reich, M. & Vasconcelos, P.M. (2015) Geological and economic significance of supergene metal deposits. *Elements* **11(5)**, 305–310.

Sandberger, F.V. (1875) Über den Clarit. *Neues Jahrbuch für Mineralogie Abhandlungen* **1875**, 382–388.

Schwinn, G. & Markl, G. (2005) REE systematics in hydrothermal fluorite. *Chemical Geology* **216**, 225–248.

Staude, S., Bons, P.D., & Markl, G. (2009) Hydrothermal vein formation by extension-driven dewatering of the middle crust: An example from SW Germany. *Earth and Planetary Science Letters* **286**, 387–395.

Staude, S., Mordhorst, T., Neumann, R., Prebeck, W., & Markl, G. (2010) Compositional variation of the tennantite–tetrahedrite solid solution series in the Schwarzwald ore district (SW Germany): The role of mineralization processes and fluid source. *Mineralogical Magazine* **74**, 309–339.

Staude, S., Göb, S., Pfaff, K., Ströbele, F., Premo, W.R., & Markl, G. (2011) Deciphering fluid sources of hydrothermal systems: a combined Sr-and S-isotope study on barite (Schwarzwald, SW Germany). *Chemical Geology* **286**, 1–20.

Staude, S., Werner, W., Mordhorst, T., Wemmer, K., Jacob, D.E., & Markl, G. (2012a) Multi-stage Ag-Bi-Co-Ni-U and Cu-Bi vein mineralization at Wittichen, Schwarzwald, SW Germany: geological setting, ore mineralogy, and fluid evolution. *Mineralium Deposita* **47**, 251–276.

Staude, S., Mordhorst, T., Nau, S., Pfaff, K., Brügmann, G., Jacob, D.E., & Markl, G. (2012b) Hydrothermal carbonates of the Schwarzwald ore district, southwestern Germany: Carbon source and conditions of formation using $\delta^{18}O$, $\delta^{13}C$, $^{87}Sr/^{86}Sr$, and fluid inclusions. *Canadian Mineralogist* **50**, 1401–1434.

Steen, H. (2013) *Bergbau auf Lagerstätten des Südlichen Schwarzwaldes*. Book on Demand, Norderstedt, Germany, 698 pp.

Stober, I. & Bucher, K. (1999) Deep groundwater in the crystalline basement of the Black Forest region. *Applied Geochemistry* **14**, 237–254.

Stober, I. & Bucher, K. (2005) The upper continental crust, an aquifer and its fluid: hydraulic and chemical data from 4 km depth in fractured crystalline basement rocks at the KTB test site. *Geofluids* **5**, 8–19.

Walter, B.F., Immenhauser, A., Geske, A., & Markl, G. (2015) Exploration of hydrothermal carbonate magnesium isotope signatures as tracers for continental fluid aquifers, Schwarzwald mining district, SW Germany. *Chemical Geology* **400**, 87–105.

Downloaded from https://pubs.geoscienceworld.org/canmin/article-pdf/57/4/427/4800215/i1499-1276-57-4-427.pdf
by University of Arizona user

Walter, B.F., Burisch, M., & Markl, G. (2016) Long-term chemical evolution and modification of continental basement brines–a field study from the Schwarzwald, SW Germany. *Geofluids* **16**, 604–623.

Walter, B.F., Burisch, M., Marks, M.A., & Markl, G. (2017a) Major element compositions of fluid inclusions from hydrothermal vein-type deposits record eroded sedimentary units in the Schwarzwald district, SW Germany. *Mineralium Deposita* **51**, 1–14.

Walter, B.F., Steele-MacInnis, M., & Markl, G. (2017b) Sulfate brines in fluid inclusions of hydrothermal veins: Compositional determinations in the system H_2O–Na–Ca–Cl–SO_4. *Geochimica et Cosmochimica Acta* **209**,184–203.

Walter, B.F., Burisch, M., Fußwinkel, T., Marks, M.A.W., Steele-MacInnis, M., Wälle, M., Apukhtina, O.B., & Markl, G. (2018a) Multi-reservoir fluid mixing processes in rift-related hydrothermal veins, Schwarzwald, SW-Germany. *Journal of Geochemical Exploration* **186**, 158–186.

Walter, B.F., Gerdes, A., Kleinhanns, I.C., Dunkl, I., Eynatten, H., Kreissl, S., & Markl, G. (2018b) The connection between hydrothermal fluids, mineralization, tectonics and magmatism in a continental rift setting: fluorite Sm-Nd and hematite and carbonates U-Pb geochronology from the Rhinegraben in SW Germany. *Geochimica et Cosmochimica Acta* **240**, 11–42.

Walter, B., Kortenbruck, P., Scharrer, M., Zeitvogel, C., Wälle, M., Mertz-Kraus, R., & Markl, G. (2019) Chemical evolution of ore-forming brines – Basement leaching, metal provenance, and the redox link between barren and ore-bearing hydrothermal veins. A case study from the Schwarzwald mining district in SW-Germany. *Chemical Geology* **506**, 126–148.

Received January 14, 2019. Revised manuscript accepted April 29, 2019.

Downloaded from https://pubs.geoscienceworld.org/canmin/article-pdf/57/4/427/4800215/i1499-1276-57-4-427.pdf
by University of Arizona user